REVIEW

Recent trends in synthesis of 2D MXene-based materials for sustainable environmental applications

Ritesh Verma[1] · Ankush Sharma[2] · Vishal Dutta[3] · Ankush Chauhan[2,4] · Dinesh Pathak[5] · Suresh Ghotekar[6]

Abstract

The unique properties of two-dimensional (2D) materials have piqued the interest of the technical community. Titanium carbide (MXene) is a member of a rapidly expanding family of 2D materials with exceptional physiochemical characteristics and a wide range of uses in the environmental field. 2D MXene has long been a topic of interest in environmental applications, including wastewater treatment, electromagnetic interference (EMI) shielding, photocatalysis, and hydrogen evolution reactions (HER) due to its high conductivity, varied band gap, hydrophilic nature, and exceptional structural stability. This study covers important developments in 2D MXene and discusses how design, synthetic methods, and stability have changed over time. In this review paper, we have discussed the strategy synthesizing of conventional, affordable heterojunctions and Schottky junctions, as well as the development, mechanisms, and trends in the deterioration of environmental organic contaminants, HER, and EMI Shielding. We also explore the obstacles and restrictions that prevent the scientific community from producing practical MXene with regulated characteristics and structures for environmental applications and analyzing its present usage. The hazardous-environmental aspects of MXene-based materials and the problems and future possibilities of these applications are also examined and emphasized. This review paper focused on environmental applications such as heavy metal detection and removal, EMI shielding, and hydrogen generation using MXenes. The issues related to wastewater, electromagnetic interference, and clean energy production are very persistent in the environment, and a better material is required to address these challenges. Thus, MXene is a kind of material that could be a better alternative to address these persistent issues, and hence, this review becomes very important, which can pave the way for the development of MXene-based materials to address these issues.

Keywords MXene · Environmental applications · Photocatalyst · EMI shielding · HER

✉ Ankush Chauhan
ankushchauhan18@gmail.com

✉ Suresh Ghotekar
ghotekarsuresh7@gmail.com

1 Department of Physics, Amity University, Gurugram, Haryana 122413, India

2 Faculty of Allied Health Sciences, Chettinad Hospital & Research Institute (CHRI), Chettinad Academy of Research and Education (CARE), Kelambakkam, Tamil Nadu 603103, India

3 University Centre for Research and Development, Department of Chemistry, Chandigarh University, Gharuan, Punjab, India

4 Centre for Herbal Pharmacology and Environmental Sustainability, Chettinad Hospital and Research Institute, Chettinad Academy of Research and Education, Kelambakkam, Tamil Nadu 603103, India

5 Department of Physics, University of West Indies, Trinidad, St. Augustine, Trinidad and Tobago

6 Department of Chemistry, Smt. Devkiba Mohansinhji Chauhan College of Commerce & Science (University of Mumbai), Silvassa, UT of DNH & DD 396 230, India

QATAR UNIVERSITY

🖄 Springer

1 Introduction

Graphene's discovery and fascinating physical features have sparked a flurry of interest in the study of 2D materials, which has led to an increase in the study of massive flat materials like transition metal dichalcogenides (TMDCs) and boron nitride. These materials are created by exfoliating the bulk 3D structure into thin 2D layers, which are connected by Van der Walls forces that are weak [1]. The remarkable electrical and optical characteristics and the mechanical properties of 2D materials eventually cleared the door for in-depth research for diverse applications over the past 10 years [2–7]. These materials also have potential as basic components in a wide range of technologies, such as membranes, layered structures, and compounds, which exhibit a wide variety of applications [8–11]. Few single-element 2D compounds have been developed, including but not limited to phosphorene, silicene, germanene, and graphene. On the other hand, the majority of such compounds consist of two or more elements, like dichalcogenides, clays, and oxides. MXenes were added to the family in 2011 by Gogotsi et al. [12]. The rapid development of several synthetic compositions has been the goal of intense scientific research in this area. Subsequently, a growing number of approximately 30 MXene-related compositions have been documented, and various others have been subject to computational investigations [13].

The unique structural characteristics of MXene can be achieved due to the addition of two transition metals. Furthermore, transition metals can create ordered 2D structures within the plane, as seen in $(Mo_{2/3}Y_{1/3})_2CT_x$, or as atomic sandwiches like $Mo_2TiC_2T_x$, resulting in a single-layered MXene with well-organized morphology. However, the ordered MXenes were created in 2014 and revised in 2015 [14]. Starting in 2017, there has been significant development of diverse MXene composites. Researchers have directed their attention toward designing structured double transition metal MAX phases and thoroughly investigating their distinctive traits, including their magnetic properties [15, 16]. Several potential MXene frameworks have been calculated using computational results on MXenes and derivatives based on their precursor [17, 18]. The formation of stable combinations on the M and X locations enables the synthesis of a considerable number of non-stoichiometric MXenes with meticulously regulated characteristics. This includes the incorporation of carbon nitrides or mixed transition metals [19]. Presently, researchers are striving to develop and integrate additional X elements into 2D boride structures. Due to the termination of hydroxyl, fluorine, and oxygen groups, the surfaces of carbonitrides are endowed with

hydrophilic properties [20, 21]. As a result of their uncomplicated processing and minimal stabilization demands, they can be transformed into films, devices, and coatings [22, 23]. Based on the observed optical bandgap of 0.9 eV for Ti_2C [13, 20] with oxygen termination, it is anticipated that MXenes will exhibit fascinating electrical and thermoelectric properties. However, Mo_2CT_x and $Mo_2TiC_2T_x$ exhibit semiconductor behavior, while $Ti_3C_2T_x$ MXene has excellent metallic conductivity [24]. Harmful waste has been produced due to the rapid growth of the global economy and industrialization over the last several decades, and this garbage has negatively affected the environment and human health. A major environmental challenge is the presence of contaminants in water streams, such as salts, heavy metal ions, medicines, aromatic compounds, and dyestuffs. For living things, the majority of them are mostly fatal and extremely destructive [25, 26]. Aerobic/anaerobic digestion, membrane filtration, adsorption, and biochar treatment are popular biological and physiochemical procedures used to remove diverse environmental pollutants [27, 28]. Nanomaterials are also becoming a cost-effective and ecologically benign choice for efficient environmental cleanup [29–31].

These very effective functional materials for environmental remediation, such as semiconductors, carbon-based nanostructures, metal-organic frameworks (MOFs), and ceramics, had improved efficiency, selectivity, mechanical stability, and sensitivity [33, 34]. $M_{n+1}X_nT_x$, where n can vary from one to three, is the formula for MXenes; here T represents surface functional groups like fluoride, oxygen, hydroxide, and chlorine, M denotes the transition metal, X represents either N or C, and x represents the total amount of these groups (Fig. 1) [35, 36]. According to the value of n in $M_{n+1}X_nT_x$, variability in MXene width is generally less than 1 nm [37].

Due to its distinctive features, 2D-MXenes have been investigated for possible applications as an EMI shielding material. Electromagnetic interference has become a constant issue in recent years due to the advancement of wireless communication technology and flexible wearables [38, 39]. The features of currently employed metal materials—susceptibility to corrosion, high density, and low flexibility—make encountering the rising EMI requirements challenging. So far, the creation of lightweight EMI shielding materials has been the endeavor of previous researchers [40, 41]. Materials that can shield against electromagnetic interference (EMI) while maintaining good flexibility and high conductivity are greatly desired, specifically if they can be conveniently manufactured into films. Due to their distinctive properties, in the upcoming generation of EMI shielding materials, MXene materials will be a formidable adversary [42, 43]. To fulfill the mechanical property demands of EMI shielding materials used in electronic products, it is of

Fig. 1 MXenes compositions as shown in a periodic table. The building blocks of MXenes are designated by color. On the bottom, you'll find schematic representations of four common MXene structures [32]
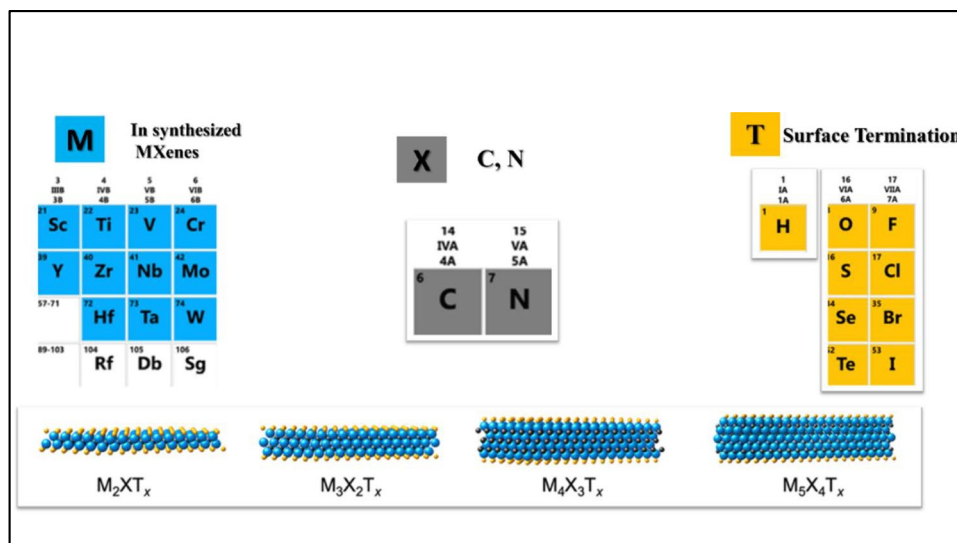

utmost importance to develop new EMI shielding materials that possess exceptional mechanical properties.

MXenes have also been a potential electrocatalyst for green energy generation and many other environment-related applications [13, 44–46]. Many people see hydrogen as a way out of the current worldwide energy dilemma and the damage it does to the environment. Hydrogen has several advantages over other energy sources, including a high energy density, the absence of pollution and greenhouse gas emissions, and the possibility of recycling. With its advantages of security, efficiency, cheap cost, durability, and environmental friendliness, it has the potential to work well in the green energy storage and conversion industries. In addition to using fossil fuels and biomass feedstock to produce hydrogen, other methods include fermenting organic waste and marsh gas. This includes the water-splitting reactions, which have shown to be a cost-effective and green option. There is a lot of research going on in this area across the world. Saxena et al. [47] showed how 2-D and 3-D MXenes could be synthesized by environmentally friendly green method and their utilization in batteries and supercapacitors. In another article, Chaudhuri et al. [48] discussed the applications of graphene oxide/MXene in supercapacitors, lithium-ion batteries, lithium-sulfur batteries, and sodium and potassium-ion batteries. Janjhi et al. [49] showed MXene-based materials to remove antibiotics and heavy metals from water. The researchers also examined the use of MXene and MXene-based materials for removing environmental pollutants, removing toxic metals, biosensors, and air purification [50–54]. These trends show that MXene and MXene-based materials are of the utmost importance, and further analysis is required. Keeping this in mind, in this review paper, we have discussed the synthesis of MXene and MXene-based materials in detail. We have also discussed

the properties of these materials, like structure, stability, electronic properties, optical properties, and magnetic properties. The review presents the application of MXene and MXene-based materials in adsorption, where the removal of organic pollutants, heavy metals, and nuclear contaminants is discussed in detail. In this way, the review is unique and presents the removal of each kind of pollutant at a single platform. Moreover, we have also shown the photocatalytic degradation efficiency of these kinds of materials, bringing a new aspect to this review. In addition, this review also presents the application of MXene and based materials for EMI shielding applications. Also, the utilization of MXene and based materials in hydrogen generation and production is discussed thoroughly. Thus, the review paper presents the solution for a major environmental challenge by bringing major portions like clean energy demand, water pollution, and electromagnetic pollution to a single platform. This review will pave the way for utilizing MXene and MXene-based materials for the various other kinds of pollution prominent in the environment. This will also pave the way for further research on these materials and their applications in different aspects of science.

In the first half of this manuscript, various synthesis techniques, the delamination process, and the most intriguing characteristics, including stability and structural, mechanical, optical, and electronic, are covered in detail. The second half of the paper is focused on promising environmental applications, including wastewater treatment (organic removal, heavy metal ions, and radionuclides), EMI shielding, and HER. The future possibilities for MXenes, which have been at the vanguard of environmental remediation, were finally projected. The development of novel MXene-based materials is projected to be a significant research area for several years owing to their remarkable characteristics

**Fig. 2** Timeline of MXene: investigation and exploration
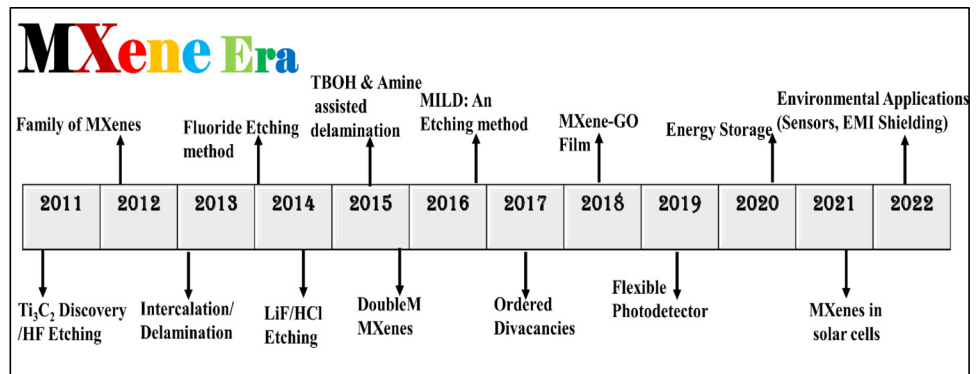
and prospective applications in the environmental field. Timeline of MXene: A journey from 2011 to 2022 is depicted by a schematic diagram in Fig. 2.

2 Synthesis of MXene

For the fabrication of MXene materials, there are diverse fabrication processes previously reported in the literature [55, 56], and one fabrication technique may be better than the other process for a particular application. Before synthesizing any material, the main goal is to engineer the material so that the resultant product has desired properties required for the targeted application. In this section, we have discussed the etching technique, delamination process, and other bottom-up techniques for fabricating MXenes, as depicted in Fig. 3. Depending upon the fabrication route followed for the fabrication process, MXenes inherit different properties. In general, the production process of MXene may require limited hours to several days, which is influenced by factors such as the etching temperature and the concentration of HF used for etching. In the case of $Ti_3C_2T_x$, for instance [57, 58], employed as little as 3 wt% of etching agent containing HF and found that the stability, purity, and characteristics of MXenes are all affected by the concentration of HF in $Ti_3C_2T_x$ flakes. For $Ti_3C_2T_x$, the technique of synthesis that is chosen has a direct impact on the end product's size, flake quality (such as the quantity and type of flaws), and surface functionalization [59]. The inherent properties and characterization methods have also been discussed in this section.

Fig. 3 Various synthesis routes to fabricate MXenes
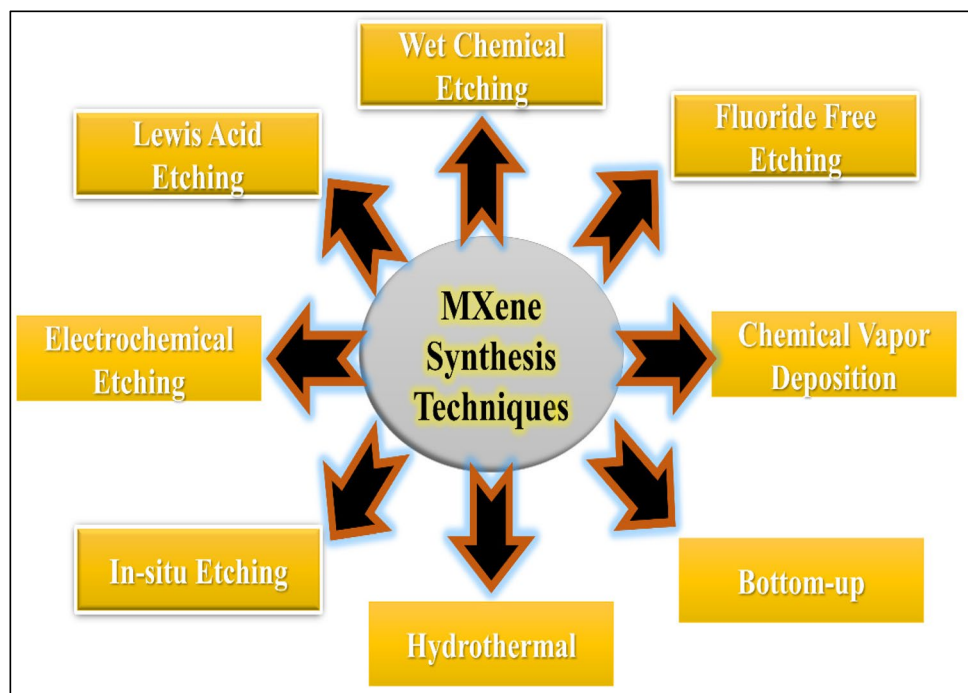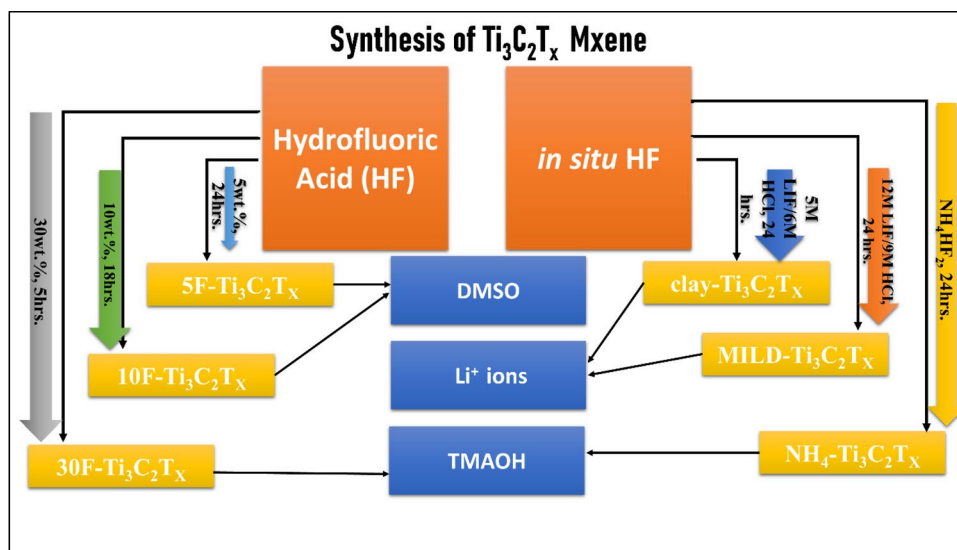
2.1 Etching

2.1.1 Etching using fluorine-containing acid

Generally, the synthesis of MXene starts with chemical etching of the MAX phase by selectively targeting a layer element, i.e., Al from Ti_3AlC_2. Through the etching process, terminated multilayered MXenes are obtained, linked by weak Van-der walls forces and hydrogen bonding [60]. The termination of MXenes with functional groups like -F, -O, and -OH can also be done while etching. The acidic solution can be removed or separated from multilayered MXenes by centrifugation after the etching process is completed. A safe pH~6 can be achieved after repeated washing of the mixture and removing reaction salts and residual acid. In order to extract multilayered MXene from the acidic solution, washing is often done through repeated centrifugation and filtration of the acidic supernatant. After this, the multilayered MXenes can be achieved by high-speed centrifugation or vacuum-assisted filtration.

The A-element layer on MAX phases is often removed selectively using HF, the most used etching agent [62]. Irrespective of quantity, it is crucial to be familiar with risk management and necessary safety procedures when dealing with hazardous HF. For the most part, the methods described in the literature, Naguib et al. used 10 or 50 weight percent of HF [63]. Despite the fact that a lower HF concentration, as will be described later enough to separate Al from Ti_3AlC_2. Naguib et al. used 30, 10, and 5 wt% HF concentrations. They demonstrated that an etching duration of 5 h is sufficient when utilizing a concentration of HF below 30% and that eliminating Al can be accomplished with as little as 5 W%, as depicted in Fig. 4. High-temperature etching and high concentrations of HF for a longer time generally lead to smaller lateral sizes and more defects in MXenes [57]. Besides HF, ammonium bifluoride and the combination of fluoride salts and acids have also been recently used as etching agents [63, 64]. It is best to avoid using a high concentration of HF because of the significant dangers associated with its extreme corrosiveness. The in situ HF approach has various benefits, including the use of less toxic substances than fluoride-based acids, intercalation, and etching processes happening simultaneously, and some researchers also found out that sonication is not required in the case of in situ etching [61, 65]. Figure 4 explains the general map toward the fabrication of Ti_3C_2 using etching acid methods like HF or in situ HF etching process. Concentrated HF has frequently been used as the preferred etchant to eliminate Al from Ti_3AlC_2, as stated in most MXene literature [66]. Previously, many researchers have used diluted HF with 5 wt% concentration to prevent the use of highly concentrated HF. Therefore, as a substitute, HF production during reaction from hydrogen fluoride or fluoride salts can be used using substances like NH_4HF_2 or LiF to create etchants with a 3–5 wt% HF content [64, 67]. Delamination methods have also been shown in Fig. 4 with different intercalating materials where sonication can also be used depending upon the application for which MXenes must be synthesized. The in situ HF etching brings more properties for MXenes than HF etching. These properties include larger interlayer distance and flake size, more -O functionalized groups, low concentration of defects, and less -F terminated groups. The lattice parameter was 2.0 when HF was used as the etchant, but it was reduced to 30–60 min when LiF/HCl was used [68]. It has also been suggested that using a greater LiF/HCl mixture lessens the need for sonication. Figure 5 is a schematic showing how MXene may be synthesized via chemical etching.

**Fig. 4** Schematic diagram showing synthesis of Ti_3C_2 MXene [61]
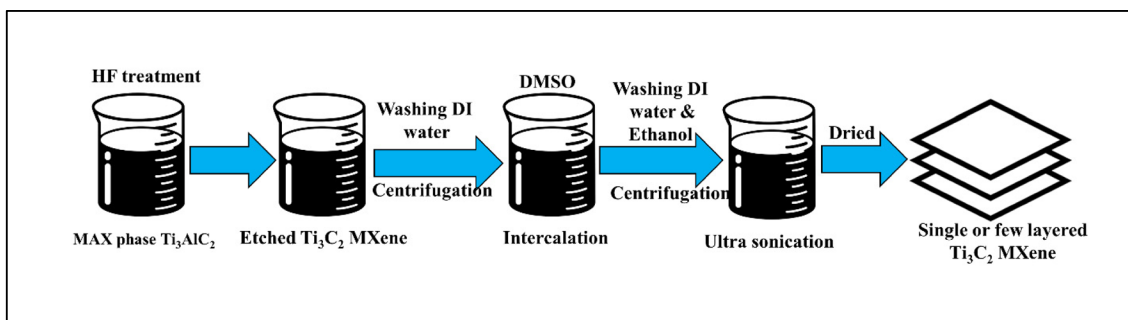
Fig. 5 Schematic representation of Ti₃C₂ MXene synthesis via chemical etching

To synthesize carbonitride and carbide MXenes, the most adaptable technique is the exfoliation of MAX in the solution containing HF. Nevertheless, in the case of the synthesis of nitride MXenes, this etching technique is usually not suggested. This is because, in HF, nitride MXenes form very high energy and have very poor stability [69]. In previously reported work, MXenes based on nitride have been synthesized by the molten fluoride salt etching method [70]. Multilayered Ti_2NT_x has been successfully synthesized previously [71].

The selective removal of Al in Ti_2AlN was attained by submerging it in a KF-HCl solution. However, this leads to the deformation in the layered structure of MXenes. To delaminate MXenes into 2D sheets, which are isolated by weakening the interaction between layers, the role of intercalating compounds has gained a huge interest. It has been considered an important step (Fig. 6). The surface area of MXenes grows when their interlayer gap expands due to the addition of ions and molecules between the layers during delamination. -F and -OH termination groups are often found in etched MXene. Following intercalation, certain functional groups in the etched MXene are replaced by cations from the intercalants, promoting the preferential adsorption of the designated contaminants [72]. In most cases, intercalating substances are utilized, and they are polar organic molecules like dimethyl sulfoxide (DMSO), urea, or hydrazine [14].
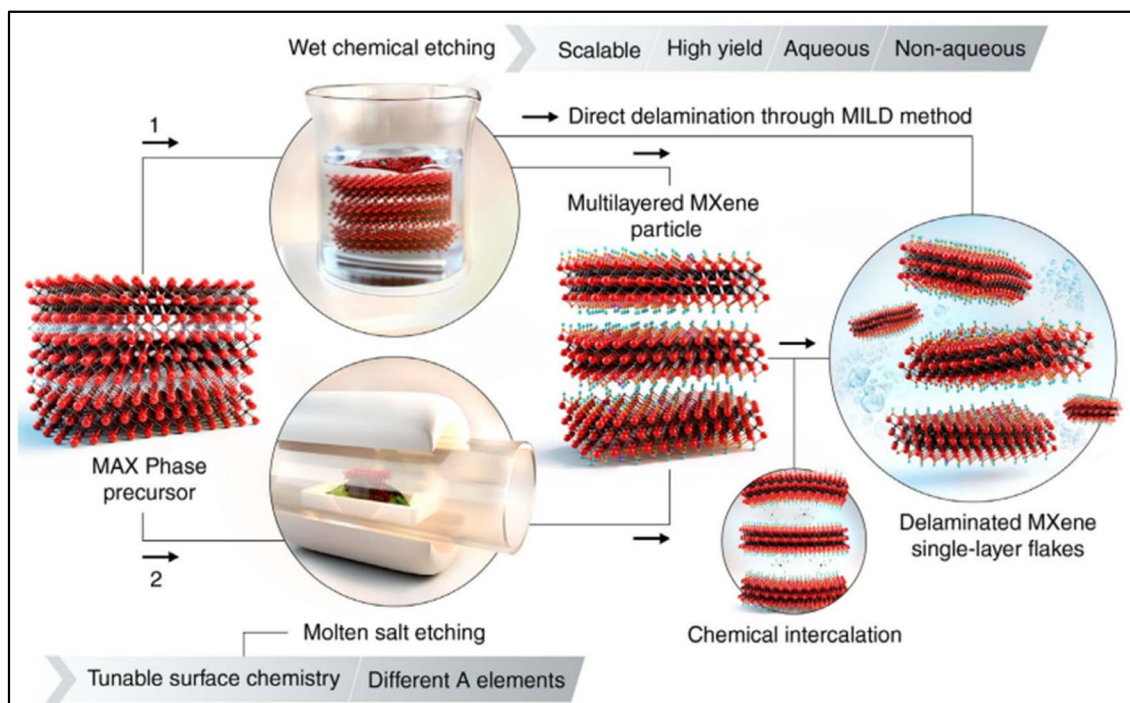
Fig. 6 Two possible strategies for extracting MXenes from MAX phases and similar layered compounds are depicted schematically here. Acids containing fluoride ions are used to selectively etch the MAX phase in the first method. Method two involves doing a selective etching in molten salts of the MAX phase. The result is often MXene particles with many layers, which can be intercalated to create monolayers [72]

Using a mechanical vibrator or ultra sonicator may create a colloidal monolayer or multilayer MXenes solution. Previous research shows that DMSO causes c-LP values to grow to 35.04±0.02 while urea decreases to 25±0.02. After ultra-sonication, the resultant dispersed 2D MXene sheets are electrically stabilized and free from aggregation and accumulation and can be processed further.

When formulating with salts based on fluorine, it becomes important to keep in mind that the efficiency, size, and capacity of Ti3C2Tx will be affected by the amount of HCl and LiF employed to produce HF during in situ process [57, 58]. Ghidiu et al. previously reported a clay method in which multilayered $Ti_3C_2T_x$ (Fig. 4) were confined into single flakes through sonication, frequently generating small and defective MXene flakes [70, 73]. In addition, a simple handshake was required to transform a multilayered powder of Ti3C2Tx into big, unbroken flakes [74]. Minimally invasive layer delamination (MILD) is the term given to this improved technique to differentiate it from the previous LiF/HCl technique. Researchers have used the MILD technique, where bigger flakes are preferred [75, 76].

### 2.1.2 Fluoride-free etching

The procedure of etching using fluoride ion acid posed environmental risks. Additionally, the fluorine-containing acid etching method can produce additional -F groups that might negatively impact environmental sustainability. This has led to the development of numerous fluoride-free etching techniques for fabricating MXenes. In this part, etching techniques based on fluorine-free salts, such as chemical vapor deposition, Lewis acidic, and electrochemical etching, have been discussed.

Alkali-based etching process has been studied previously by many researchers due to the amphoteric character of Al [77, 78]. Organic bases like n-butylamine or tetrabutylammonium hydroxide (TBAOH) might deteriorate the interactions among M-X layers, as was found by Naguib et al. [61]. They are thus advantageous for the widespread

delamination of stacked MXenes. The above intercalated MXenes had shortened source material in -F groups as well as broad d-spacing [61]. In order to specifically target Allayers, $Al(OH)^{4-}$ reconfigured and TMA^+-intercalated T_3C_2 resulted from TBAOH's use as an intercalation agent by Xuan et al. [79]. In order to create Ti_3C_2 with a distinctive hierarchical highly porous, the conjunction of ball milling was done using etching based on organic bases [80]. Despite the fact that these techniques for etching remove the creation of -F end groups, the significant amount of base necessary for the process still poses a considerable risk, thereby limiting its widespread use in manufacturing.

Many researchers have reviewed electrochemical etchings previously [81, 82]. One of its benefits is the electrochemical etching process's relatively quick etching time. Typically, the electrochemical etching method requires two phases: targeted removal of the Al layer from an electrode is accomplished by either (1) electrochemical etching or (2) hydrolysis to produce a MAX phase predecessor with reduced lateral parameters [83]. Additionally, Yang et al. created a simple approach that relies on a lithiation intercalation alloying-expansion-micro explosion process to generate single or small layers of $Ti_3C_2T_x$ MXene [84]. A general method for etching MAX phases that have been published by Li et al. [85]. The process of production is parallel to the etching based on fluoride-based salts. In the MAX material, the M atoms are coordinated with Lewis salts cations and Cl^- ions that function as H^+ and F^- ions, respectively. In addition to chemical vapor deposition, wet etching has been investigated to make MXenes [86, 87]. Scanning electron microscopic images of the compact layered structure of Ti_3AlC_2 powder and $30F-Ti_3C_2T_x$ are depicted in Fig. 7. SEM image displays the compact layered structure of Ti_3AlC_2 powder and the multilayered $30F-Ti_3C_2T_x$ powder created with 30 wt% HF. Thus, it can be concluded that the variation in the etching process and various methods can produce variation in the morphology of the MXene layers.

Fig. 7 SEM images of **a** display the compact layered structure of Ti_3AlC_2 powder, and of **b** illustrate the multilayered $30F-Ti_3C_2T_x$ powder created with 30 wt% HF, highlighting MXene layers that are expanded and exhibit an accordion-like structure when viewed at higher magnification [88]
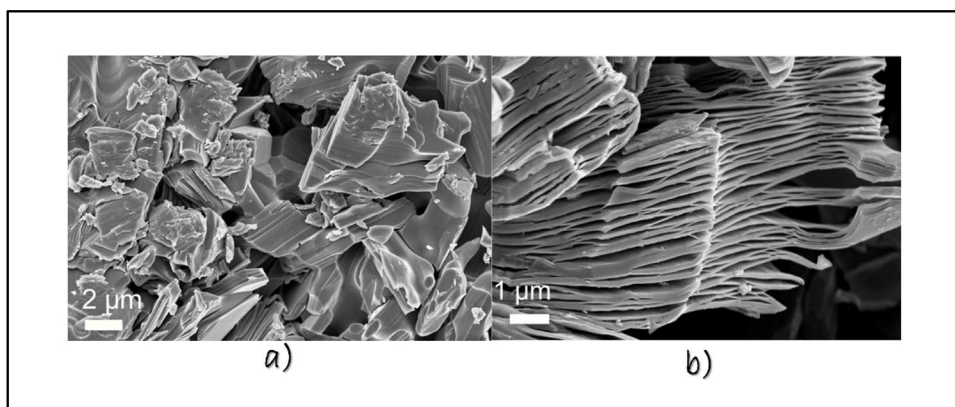
2.2 Bottom-up techniques

As was previously mentioned, MXene materials are often fabricated using selective etching processes. The template approach, atomic layer, and chemical vapor deposition (CVD) are only a few bottom-up processes that have emerged in recent years [89, 90]. Bottom-up procedures, especially chemical vapor deposition (CVD), produce materials with superior crystalline purity to those produced by selective etching techniques. These approaches have only synthesized multilayer ultrathin films rather than single-layered MXenes [91]. By using magnetron sputtering to deposit elements like Ti, Al, and C onto a sapphire substrate, Halim et al. successfully created a thin-film Ti_3AlC_2 MAX phase. In addition, direct magnetron sputtering can be used to create both non-MAX (Mo_2Ga_2C) and MAX phase (Mo_2GaC) thin films, which can then be used to synthesize epitaxial Mo_2C films via straightforward selective chemical etching. Another novel method for directly synthesizing MXene materials is chemical vapor deposition (CVD) [90]. For instance, CVD synthesis using methane over an alloyed surface containing Cu and Mo above 1085 °C yielded ultrathin -Mo_2C having high quality [87, 89]. Using chemical vapor deposition (CVD), Lipatov et al. have recently manufactured thin flakes of $Ti_3C_2T_x$ [92].

Template techniques for creating 2D MXene materials have also been developed previously by many researchers [93]. Using the template method, Joshi et al. fabricated an MoN film having a hexagonal structure [93]. Jia et al. utilized the dicyandiamide dopant and MoO_2 template to synthesize N-doped Mo_2C (N-Mo2C) in an ultrathin form [94]. In order to manufacture different MXene films and subsequently analyze their mechanical, optical, and electrical properties, it is crucial to do further research into these bottom-up procedures.

2.3 Intercalation methods

To break down MXene into separate 2D sheets, intercalation materials have been used to weaken the bonds among the interconnected layers and to widen the interlayer distance between the flakes of MXenes [61]. A proper solvent is required for the intercalation and delamination, and procedure. Also, a stage is included to mix the intercalant into 2D MXene sheets, particularly ultra-sonication, that determines the concentration and size of the flakes. After that, the solution is centrifuged to remove the intercalation material from the multilayered MXene [94]. Functional and processable 2D sheets of MXenes, which are electrically stabilized, also free from clumping and aggregation, are obtained in the final colloidal solution. Besides, the targeted application, the etching method, and the concentration required will decide whether sonication is needed. Long-time sonication with high power leads to smaller flake sizes having defects and different concentrations than the non-sonicated solutions. The type of intercalated material used and the synthesis process determine the concentration of MXene sheets in the solution. Following are some reports on previously used intercalation materials and their effect on the delamination of MXenes:

Dimethyl sulfoxide: dimethyl sulfoxide (DMSO), a type of large organic molecule, was among the initial intercalants used to expand the spacing between the layers in $Ti_3C_2T_x$ synthesized using fluorine-based salts [95]. $Ti_3C_2T_x$ may also have DMSO or another organic solvent added to it. Without ultrasonic treatment, the stacked sheets of $Ti_3C_2T_x$ will settle to the bottom of the vial when DMSO or other organic solvents are used to dissolve them. When using these techniques, flake sizes typically range from a few hundred to a few thousand nanometers.

Tetraalkylammonium hydroxides: TBAOH and TMAOH are two examples of tetraalkylammonium compounds used to exfoliate oxides with a layered structure [96]. Multilayer oxides and other materials can be delaminated with this method based on the ion exchange leading to delamination and expansion with just a shaking process [96]. MXenes Nb_2C, V_2C, Mo_2C, and Ti_3CN have all been exfoliated using TBAOH. On the other hand, even ultra-sonication was ineffective in TBAOH delaminating $Ti_3C_2T_x$ [61]. Other research claims that by first treating the MXene surface with twenty to thirty wt% HF for a short time, $Ti_3C_2T_x$ can be produced and exfoliated employing TMAOH [79]. Since the breakdown temperature of TMAOH is more than 200 °C, a greater degree of heat is necessary to eliminate the intercalated substances [97, 98].

Lithium ions: Using lithium-containing etchants leads to delamination caused by the intercalation of Li^+ ions. Although sonication of the intercalated MXene is considered necessary for the clay approach but not for the MILD method, as shown in Fig. 4. These flakes are bigger and more defect-free than those produced by sonication. Since the MILD approach produces flakes directly proportional to the shape and grain size of the beginning precursor powder, the MXene synthesis process is top-down. That is why larger MXene flakes require larger crystals of MAX phases.

3 Properties

3.1 Structure and stability

Novel stable compounds are often highlighted using computer modeling to examine their structural characteristics.
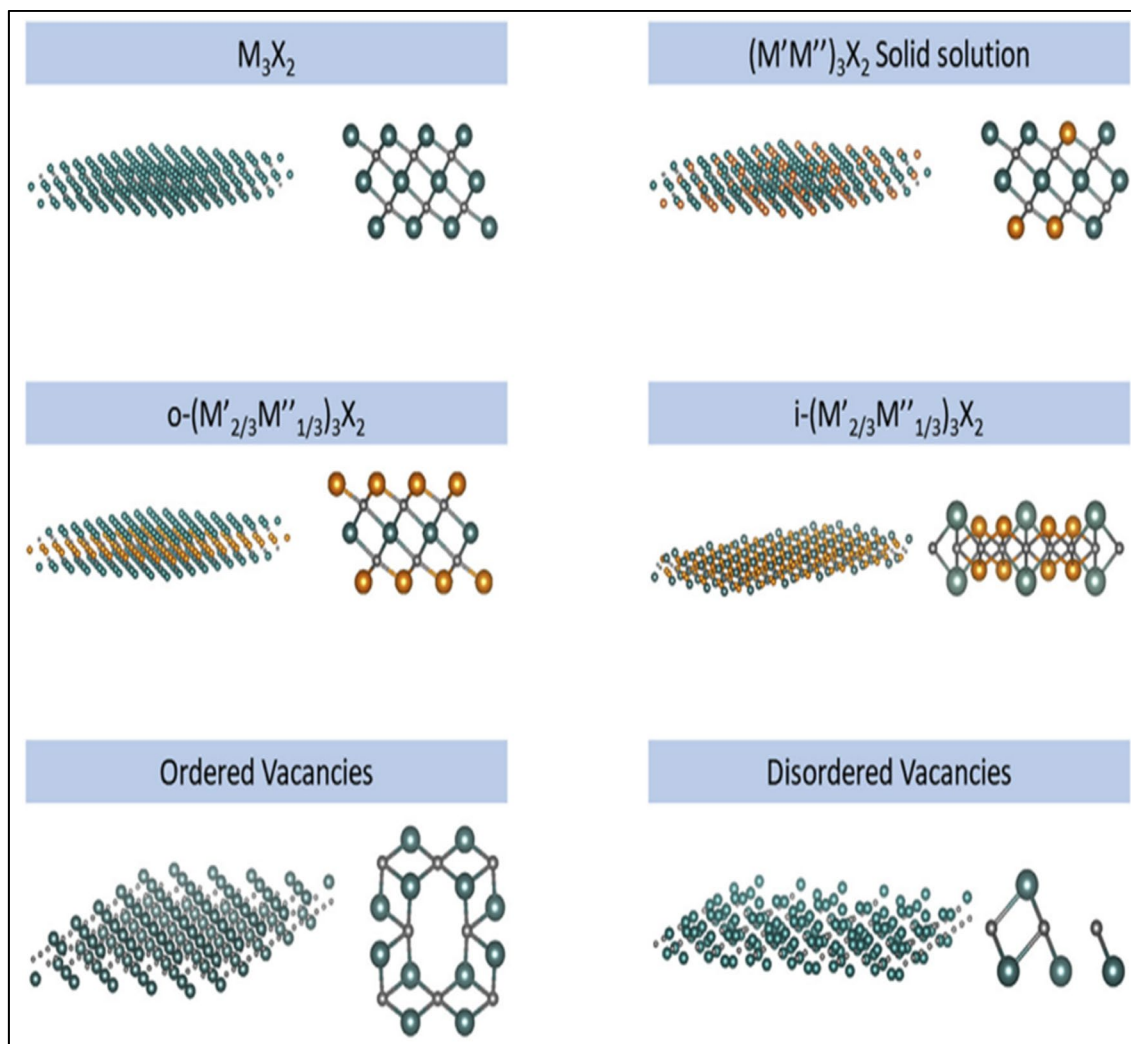
Fig. 8 Different forms of MXene structures. Reprinted with permission from [99] (Elsevier, License No. 5435971332920)

These studies revealed that there are six distinct forms of MXenes, as shown in Fig. 8: (1) solid solutions; (2) single-M elements; (3) double-M elements that are out-of-plane ordered with the transition metals occupying the outer layer; (4) in-plane ordered; (5) ordered vacancies; and (6) randomly distributed vacancies [100–103]. The structure of MXenes remains like MAX (Fig. 9).

MXenes' characteristics and stabilities may be modified by their terminal groups. The impact of different functional groups and configurations has been described in only a handful of publications [105]. Six bonds between X and M atoms produce M_2XT_2; this has been confirmed by computational research [106]. This is the signature six coordination of transition metals. When comparing the positions of the terminated T atoms to those of the X and M atoms, it was discovered that diverse configurations were often the most stable [107]. In certain MXenes, to improve their electrical interface, the T elements were sited above the X

atoms [108]. Experiments confirmed that, as predicted by DFT calculations, termination groups in V_2CT_x and $Ti_3C_2T_x$ MXenes are distributed randomly.

Experimental methods for studying the MXenes structure have included scanning tunneling microscopy (STM) with atomic precision and high-resolution transmission electron microscopy [109, 110]. The structure of MXenes, along with data on their termination groups and intrinsic defects, was all gleaned from these methods. The stoichiometric composition and elemental ratio were also investigated using XPS [111]. NMR spectroscopy has previously been used in certain research to learn about functional groups on MXenes' surfaces.

Since studies suggested that MXenes might degrade following exposure to moisture or higher temperature, it is important to discuss the durability of MXene materials during storage and application [112]. Extensive research on Nb_2CT_x, for instance, has led researchers to postulate that
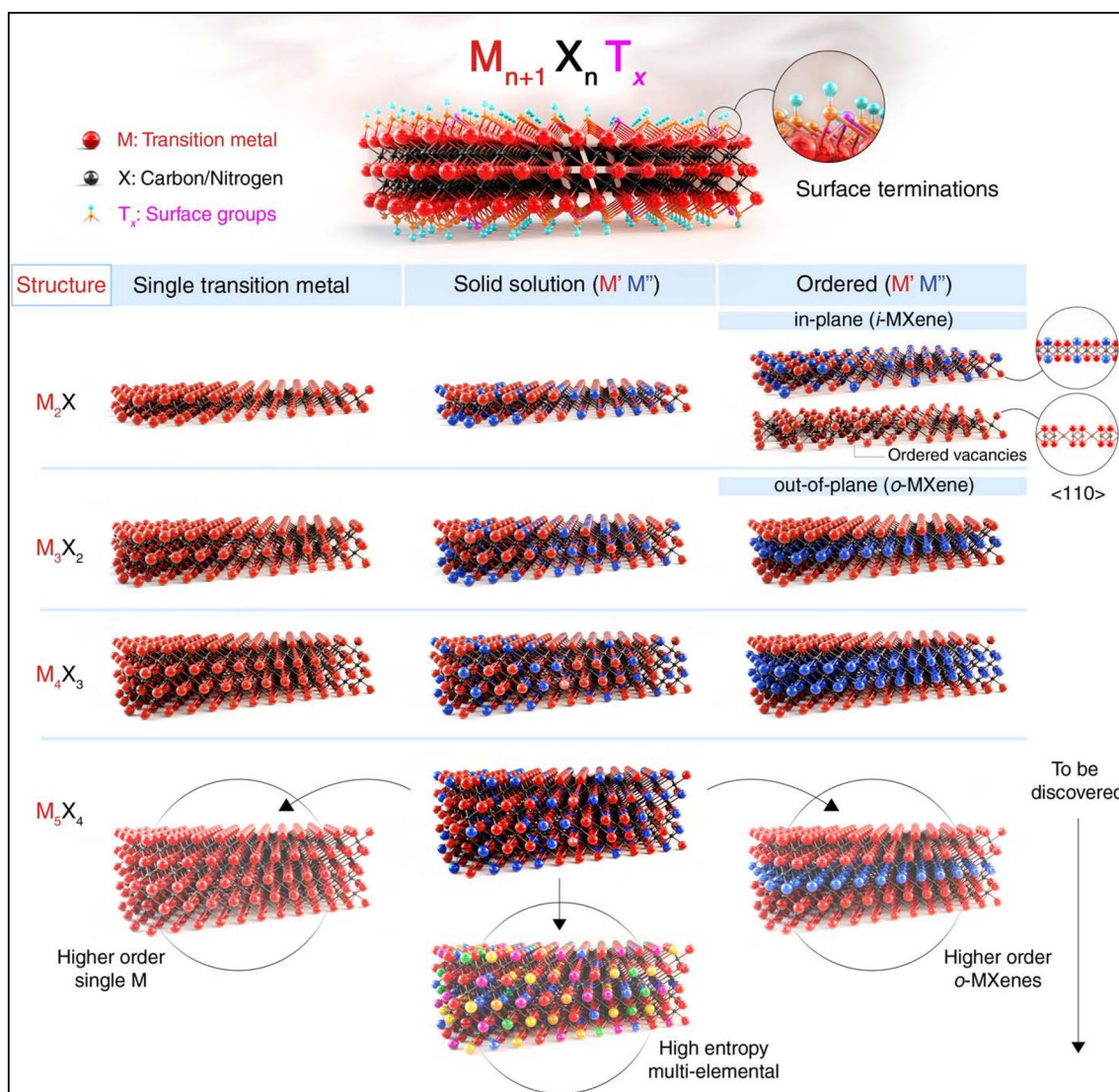
Fig. 9 Schematic illustration of the structure of MXene [104]

the structure destabilizes and deteriorates because Nb atoms located at hcp surface locations interact with the exposed oxygen [113]. Even more so, Lipatov et al. estimated that $Ti_3C_2T_x$'s initial conductivity would decrease by 20% after being exposed to air for more than 70 h [43]. Therefore, to prolong the shelf life of manufactured MXene materials, it is suggested that they be kept in a phenomenon having no oxygen, dissolved in a powerful polar solvent, or filtered using a process such as MXene films [106]. Additionally, the stability of MXene can be enhanced by using optimized etching procedures that reduce the number of adatoms on its surface.

Because each OH/F surface functional group can be eliminated at a distinct operating temperature, thermal treatment has been recommended as a possible strategy for their efficient complete removal [114, 115]. Previously, $Ti_3C_2T_x$ was

heated to 750 °C in a vacuum by Persson et al. [116]. As a result of this method, a pure MXene product can be prepared by removing the majority of the oxygen-based terminations. More research is needed to determine the thermal characteristics in air and oxygen environments before they can be used in real-world applications. Although rutile crystals are produced at roughly 500 °C in an oxidative environment, the phase transformation occurs at a significantly higher temperature (for instance, $Ti_3C_2T_x$ has converted to TiC at 1000 °C calcination over 2 h). While Mo-based MXenes have recently demonstrated thermal stabilities up to 530 °C, $Zr_3C_2T_x$ has demonstrated greater (1200 °C) thermal stability relative to $Ti_3C_2T_x$, allowing it to be used in a number of applications [116, 117].

The MXene characteristics can be drastically changed based on the environment and method of creation. Only

one study that compared the thermal characteristics of $Ti_3C_2T_x$ prepared using two distinct methods was identified. The results indicated that MXene synthesized with NH_4HF_2 intercalating agent exhibits a transition temperature higher than the one made through the HF route [118]. However, additional research into alternative approaches is still needed.

3.2 Mechanical properties

The terminations present in MXenes have a significant impact on their mechanical characteristics. The toughness of MXenes with a -O group is generally greater. MXenes display less elastic stiffness with -F and -OH groups than those with -O groups [119]. This may be because the lattice parameters of MXenes with -O functional terminations are usually smaller than those with -OH or -F functional groups [120]. The versatility of MXenes doped with surface functional groups was greater than that of pure MXenes. For instance, Guo et al. [121] demonstrated that the surface functionalization of Ti_2C MXene decreases the material's Young's modulus but increases its ability to withstand strain than pure graphene and MXene. Upon tensile stress, the surface termination in Ti_2C shields the material from damage, preventing the layers of Ti from collapsing and increasing the material's critical strain.

The atomic layer count (n) in MXene ($M_{n+1}Xn$) also affects its mechanical characteristics. According to Borysiuk et al. [122], the toughness and durability of surface-functionalized $M_{n+1}X_nT_x$ are improved as n is decreased. Elastic constant and Young's moduli of MXenes were calculated by Yorulmaz et al. [123] with the use of classical

molecular dynamics in their pure form. To improve their compressive and tensile capabilities, stiffness, and versatility, MXenes can be mixed with other polymers [33, 73]. Polyvinyl alcohol (PVA)-$Ti_3C_2T_x$ composites, for example, exhibited remarkable malleabilities and excellent tensile and compressive capacities. The study demonstrated that the $Ti_3C_2T_x$-PVA composites had a tensile strength of approximately 4.1 times larger than $Ti_3C_2T_x$, because of the interfacial interaction between the two materials [124]. The Ti_3C2Tx-UHMWPE material has advantages as well. It has been observed that polyethylene and $Ti_3C_2T_x$-PAM have higher yield strength and toughness [125, 126].

3.3 Electronic and optical properties

The electrical characteristics of MXenes were found to be influenced by both the termination groups and the transition metal element. Altering the terminations could result in a transition of the MXene from a metallic state to a semiconductor or even a topological insulator [127]. Most MXenes exhibit metallic behavior when surface functional groups are introduced. Work functions (WF) of MXenes are shown in Fig. 10, as calculated because of the modification of functional groups [129]. Compared to pure MXene, MXenes with a -OH group have a greater WF, while MXenes with a -O group have a small work function [130]. -F functionalized MXene decorations exhibit a paradoxical pattern typical of this class of materials. The shift in WF values was mostly due to the effect of the termination on the dipole moment. The WF was found to be reduced for the -OH functional group and increased for the -O group, both of which resulted

Fig. 10 Image depicting work function of bare MXene, Pt, and Sc decorated with functional groups [128]
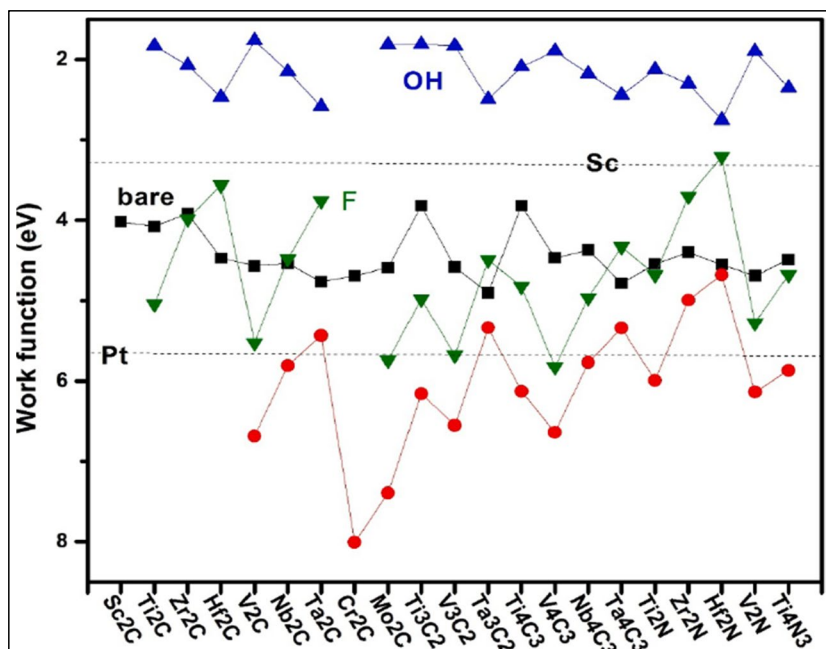
in a negative dipole moment. Different MXene materials will exhibit positive or negative dipole moments for the -F group. The MXene WF value would be dragged down to the intermediate level by the interaction of -OH, -O, and -F groups [131]. A close correlation exists between the etching and delamination processes used to synthesize MXenes and their conductivity. The conductivity of MXenes is subject to modification by intercalated species and the interaction between the nanosheets. For instance, the conductivity of Mo_2CT_x would decrease if TBAOH was inserted during the synthesis process, as this would result in TBA^+ intercalated species among the MXene layers, leading to lower conductivity. Applying heat treatment can eliminate TBA^+ species, leading to a reduction in the interlayer distance and a consequent enhancement in conductivity [116].

The absorbance of ultraviolet (UV) and ultraviolet-visible (UV-vis) light, specifically, is closely linked to the photocatalytic activities of MXenes. The transmission was significantly affected by the thickness and intercalation of the MXene layer. The 5-nm-thick $Ti_3C_2T_x$ films described by Hantanasirisakul et al. [128] had up to 92% transmission in the ultraviolet-visible spectrum between 300 and 500 nm. After exposure to urea, hydrazine, and DMSO, the transmittance of $Ti_3C_2T_x$ decreased. However, intercalation of $Ti_3C_2T_x$ with tetramethyl ammonium hydroxide or NH_4HF_2 increased transmission. Furthermore, MXenes' transmission property was significantly different from that of the MAX phase predecessor. Compared to $Ti_3C_2T_x$ (90%), the transmission of the MAX phase in Ti_3AlC_2 was only about 30% [64]. Researchers found that the surface functionalization of MXenes affected how well they absorbed light. Compared to the light absorption properties of -OH and -F functionalized Ti_2C and Ti_3C_2, pure, -O functionalized Ti_2C and Ti_3C were superior [119].

3.4 Magnetic properties

Studies have expanded their assessments to MXenes' magnetic characteristics because of the magnetization possibilities, in contrast to MAX phases. Ti_3N_2 [132], Zr_3C_2 [133], Ti_3CN [134], Cr_2C [135], Fe_2C [136], Zr_2C [133], and Ti_4C_3 [70] are just a few examples of the purified compounds that are hypothesized to have magnetic moments. However, each MXene and functionalization group must be examined separately following functionalization. For example, Cr_2NT_x and Cr_2CT_x maintain ferromagnetic at normal temperature with terminated attached [137], whereas Ti_3CNT_x and $Ti_4C_3T_x$ get to be losing the magnetization with the terminations [134], and Mn_2NT_x is ferromagnetic irrespective of the surface functionalization [138]. Previously reported magnetic moments, nonetheless, are still just computer simulations and have not yet been seen in an experimental setting. This is because there is currently a deficiency of control over surface chemistry and inadequate production of pure MXenes [139].

4 Environmental applications

4.1 Adsorption

4.1.1 Removal of organic pollutants

The most important category of aquatic pollutants is organic contamination, distinguished by increased chemical stabilization and tolerance to biological deterioration. The main aqueous organic pollutants include a variety of dyestuffs, phenols, medicines, and insecticides [140–146]. The occurrence of these organic pollutants immediately impacts our ecology in wastewater. Therefore, it is crucial to remove these organic pollutants properly.

Table 1 MXene-based composites for organic removal

Organic compound	Adsorbent	Results	Reference
Methylene blue	Ti_3C_2-COOH/(PEI/PAA)$_n$	Electrostatic attraction led to higher adsorption capacity	[147]
AMT	Sonicated $Ti_3C_2T_x$	Increased functional groups lead to enhanced performance	[27]
RhB and MB	Ti_3C_2 - Co_3O_4	Homogeneous dispersion of NPs prevented the restacking of sheets which led to higher adsorption capacity	[148]
Phenol	$Ti_3C_2T_x$	Experimental data was fitted by Langmuir isotherm and pseudo-first-order model as suggested by isotherm studies	[149]
MB	Ti_3C_2@Fe_3O_4	pH was optimized around 3 or 11 for optimized adsorption capacity	[150]
Formaldehyde	$Ti_3C_2O_2$	Adsorption energy~.45eV resulted in the adsorption	[151]
MB	Ti_3C_2 - SO_3H	Langmuir isotherm adsorption model	[152]
Urea	$Mo_2TiC_2T_x$	Interlamellar space was easily occupied by the urea molecules	[153]
MB	V_2CT_x	Electrostatic attraction led to the higher adsorption capacity	[154]
MB	NaOH–$Ti_3C_2T_x$	Adsorption properties were enhanced by the alkaline treatment	[155]

Recent studies on the adsorption of pollutants, like urea, amitriptyline (AMT), AB80, phenol, and methylene blue, by materials based on MXene have been conducted through a small group of researchers. The most current adsorption of organic pollutants employing different MXene-based composites is summarized in Table 1. An example of MXene production was given by Meng et al., who used the in-situ technique to synthesize MXene [156]. Wu et al. [149] reported that $Ti_3C_2T_x$ displayed exceptional adsorption capabilities towards phenol, with recyclability demonstrating excellent duplicability and long-lasting sustainability. The charged state of organic contaminants significantly impacts the adsorption kinetics of MXene compounds. The adsorption of multiple pharmaceutical compounds, including 17-ethinyl estradiol, diclofenac, carbamazepine, ibuprofen, AMT, and verapamil, was conducted for the first time by Kim et al. [27] using $Ti_3C_2T_x$ under three different solution pHs.

Moreover, MXenes have demonstrated remarkable adsorption capabilities toward various types of dyes. Wei et al. [155] inspected the adsorption behavior of methylene blue using pure $Ti_3C_2T_x$ and three different alkaline-treated $Ti_3C_2T_x$ MXenes. Their research indicated that $Ti_3C_2T_x$ treated with NaOH displayed an adsorption capacity of around 189 mg/g, more than the other layered two-dimensional materials [156]. Fe_3O_4 was painted onto the Ti_3C_2-MXene surface by Zhu et al. and used as an adsorbent toward MB dye at various temperatures [152]. Their studies showed that, owing to hydrogen bonding and strong electrostatic contact between Ti-OH and MB, the adsorption capacity of $Ti_3C_2T_x$ increased with an increase in temperature [152]. Adding terminated groups containing sulfone also significantly improved the adsorption capacity of $Ti_3C_2T_x$ [157]. The etching method used to produce MXenes also affects their adsorption efficiency. Hydrothermally produced Ti3C2 showed a higher ability to bind MB dye than the conventional etching method based on fluorine-based salt, likely due to the larger specific surface area created by the hydrothermal method [147]. Self-assembled Ti_3C_2-Co_3O_4 MXene nanocomposites were found to effectively adsorb RhB and MB dyes, while $Ti_3C_2T_x$ MXene coupled with terephthalate showed a high adsorption capability against MB, conceivably due to the accessible carboxylate groups and greater separation between MXene [158].

4.1.2 Heavy metal removal

Elements with a density of more than 5g/cm^3 and high atomic weight of up to 200 come under heavy metals [159]. The release of industrial waste into the water sources results in excess heavy metals in the environment. Heavy metals do not have the properties of degradation and incline to gather in living organisms. Cr, Pb, Ni, Hg, Zn, Cd, As, and Cu are frequently discovered heavy metals in industrial wastewater [160]. MXenes demonstrated the ability to adsorb different heavy metal ions from industrial effluent effectively.

One of the significant advantages of MXene nanosheets in capturing heavy metal ions is their small interlayer gap, which is less than 2Å, making them suitable for capturing heavy metal ions [161]. Moreover, the adsorption performance of MXenes was enhanced by surface-functionalized characteristics. Titanium-based MXenes, particularly $Ti_3C_2T_x$ nanosheets, are the most commonly used adsorbents for heavy metal ions. Table 2 discusses the MXene-based composites for heavy metal removal. Ti_3AlC_2 is exfoliated by Fard et al. [161] to create $Ti_3C_2T_x$ nanosheets, used to adsorb barium ions. MXenes also have the unique ability to remove pollutants via an in situ reduction-adsorption method. In addition to removing the reduced Cr(III) ions, $Ti_3C_2T_x$ alongside reduced Cr(VI) ions Cr(III) [171]. Delaminated $Ti_3C_2T_x$ MXene nanosheets were used in a different study to use the reduction-adsorption method to remove

Table 2 MXene-based composites for heavy metal removal

Heavy metal ion	Adsorbent	Results	References
Ni(II)	$Ti_3C_2T_x$/LDH	The adsorption behavior was described by pseudo-second-order kinetics	[162]
Pb(II)	$Ti_3C_2T_x$	Higher negative surface charges resulting in higher adsorption capacity of MXene than graphene	[163]
Hg(II)	$Ti_3C_2T_x$/Fe_2O_3	Negatively charged surfaces and -O and -OH groups lead to high adsorption capacity	[164]
Cu(II)	$Ti_3C_2T_x$	Pseudo-second-order kinetics explains the Cu uptake	[165]
Cr(VI)	$Ti_3C_2T_x$	80mg of Cr(VI) was removed	[166]
Pb(II); Cu(II)	$Ti_3C_2T_x$/alginate composites	After cross-linking there was no loss in performance	[167]
Ba(II)	$Ti_3C_2T_x$ and Alk-$Ti_3C_2T_x$	3.1 times adsorption than pristine $Ti_3C_2T_x$	[168]
Pb(II)	$Ti_3C_2(OH/Ona)_xF_{2-x}$	High adsorption capacity	[169]
Cd(II)	Alk-Ti_2Csheet	Improvement in Cd adsorption than bulk counterpart	[170]
Cr(VI)	$Ti_3C_2(OH)_{0.8}F_{1.2}$	MXene got functionalized with -F group	[74]

جامعة قطر
QATAR UNIVERSITY

Springer

Cu(II) ions [172]. Ti$_3$C$_2$T$_x$ MXene was also effectively used by Pandey et al. [173] to convert BrO$_3$ ions in water to Br.

The surface-functionalized properties of MXenes were found to impact the capability to adsorb heavy metals. Researchers created Ti$_3$C$_2$(OH/ONa)$_x$F$_{2-x}$ with an OH group to remove Pb(II) from wastewater [167]. The MXene exhibited a high Pb(II) ion removal capacity, and the symmetry for adsorption-desorption was touched in less than 2 min. Additionally, the sorption capability of Ti$_3$C$_2$T$_x$ for Pb(II) ions was further enhanced by terminating with a coupling agent silane coupling, increasing to 147.3 mg/g.

Additionally, MXene compounds have effectively removed several heavy metal ions through adsorption. Hybrid Fe$_2$O$_3$/Ti$_3$C$_2$T$_x$ blends were created by Shahzad et al. [164] and cast off to remove mercury ions. C-TiO$_2$ composites MXene were compared for their ability to absorb Cr(VI) ions by Zou et al. [174]. Similar improvements in Cu(II) ion elimination from wastewater were also seen in the levodopa-decorated Ti$_3$C$_2$T$_x$ MXene-based films also capable of eliminating Au(III), Pd(II), Ag(I), and Cr(VI) ions [175]. These were reused after being cleaned with HCl and NaOH solution.

4.1.3 Removal of nuclear contaminants

The pollution brought on by nuclear waste has drawn attention due to the nuclear industry's rapid expansion due to its detrimental environmental consequences. Chemisorption is still the most popular and efficient way to handle the detoxification of nuclear waste out of all the methods for dealing with it. MXenes have distinguished themselves among the various adsorbents used to detoxify nuclear waste as being particularly effective against the adsorption of Cs+, palladium, Th(IV), and uranium U(VI) [176, 177]. Both experimental results and theoretical predictions made using DFT calculations were published for the efficient removal of uranyl ions by V$_2$C(OH)$_2$ nanosheets [178, 179]. The elimination of U(VI) ions by the V$_2$CT$_x$ nanosheets was exceptionally high (174 mg/g). However, the sorption capacity of V$_2$C(OH)$_2$ nanosheets, as estimated by DFT, was substantially greater than the actual value (89.9 mg/g) [178].

Using the hydrated intercalation approach, Wang et al. [180] created DMSO intercalated Ti$_3$C$_2$T$_x$ nanosheets to remove uranium ions. The investigational outcomes revealed that the adsorption capacity increased significantly up to 160 mg/g due to hydration and intercalation stimulation. In an alternative study, Wang et al. [181] reported similar observations using Ti$_3$C$_2$T$_x$ MXene to remove U(VI) via reduction adsorption techniques. The hydrated-Ti$_2$CT$_x$ MXene displayed stronger specificity and sorption capability against Ti(IV) ions than the dry-Ti$_2$CT$_x$, according to research by Li et al. [182]. According to the sorption mechanism analysis, ion exchange and electrostatic contact were the primary mechanisms for removing radionuclides, as shown in Fig. 11. In addition, Ti-OH and Th(IV) exhibit a high affinity, according to their XPS study.

Mu et al. [184] fabricated Ti$_3$C$_2$T$_x$ by treating it with a fluorine-based salt process, exfoliating it at various

Fig. 11 Adsorption isotherm of methane over Ti$_3$C$_2$ manufactured by using HCl from 0 to 60 bar and at 25°C: (1) LiF, (2) NaF, (3) KF, and (4) NH$_4$F. Reprinted with permission from [183] (Elsevier, License No. 5435980355724)
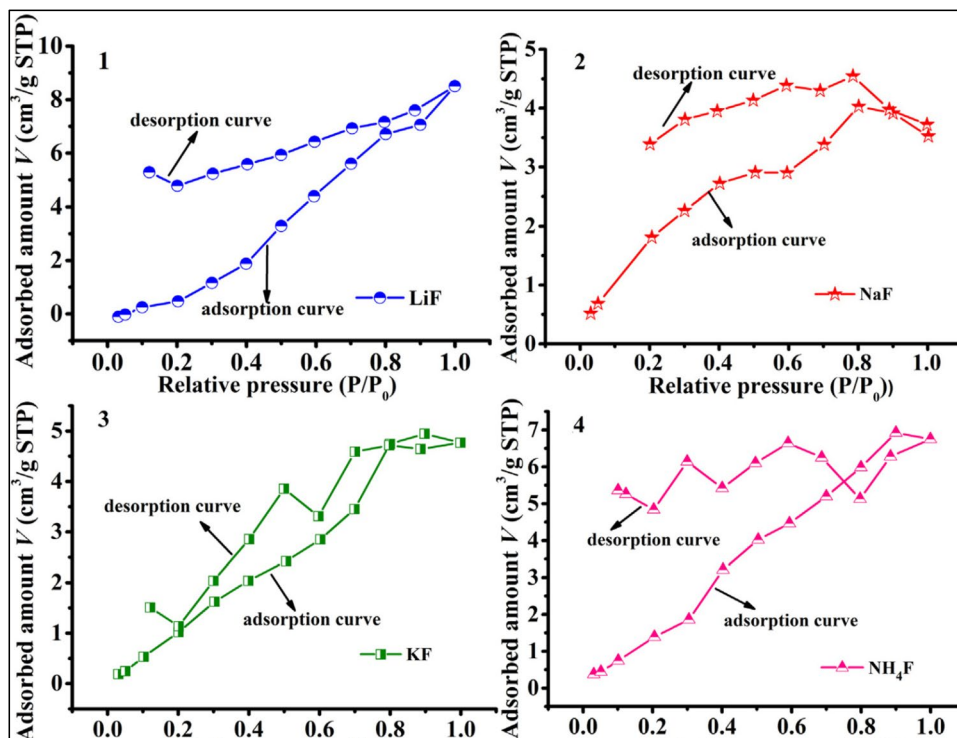
temperatures, and using it as an adsorbent for Pd(II). Their outcomes indicated that the samples that underwent more intense exfoliation at higher temperatures had advanced adsorption capacities and good regeneration characteristics. Hierarchical titanate nanostructures (HTNs) were created from MXene using an enhanced hydrothermal oxidation and alkalization method by Zhang et al. Hierarchical titanate nanostructures had a higher adsorption capacity for europium ions, primarily due to ion swapping with the terminating groups at the interlayer. MXenes also efficiently remove Cs+ ions from wastewater [177, 179]. As shown in Fig. 11 (2), $Ti_3C_2T_x$ nanosheets quickly reached equilibrium. The improved adsorption ability was attributed to the MXene having layers and the terminating groups attached. Recent research by Jun et al. [176] associated eliminating radioactive cesium ions from nuclear wastewater using porous activated carbon and $Ti_3C_2T_x$. The greater amount of surface negative charges on MXene than on PAC was thought to be responsible for its higher adsorption capability. The suggested removal mechanism involved electrostatic contact between the adsorbent and the cesium ions.

Wang et al. [185] reported the development of a new 3D structured Ti_2CT_x composite to eliminate perrhenate better. They incorporated poly(diallyl dimethylammonium chloride) to adjust charges at the surface and enhance Ti_2CT_x stability, efficiently eliminating rhenium up to 363 mg/g. In a different investigation, Deng et al. [186] created nanocomposites of $Ti_3C_2/SrTiO_3$ by partially oxidizing a multilayered Ti_3C_2 based on hydrothermal crystallography. These materials were then used to remove U(IV) ions.

4.2 Photocatalytic degradation

With CO_2 and H_2O as the end products, photocatalysis, a powerful and affordable photo-redox method, has demonstrated tremendous potential in wastewater purification from many organic contaminants [187]. In order to develop the pot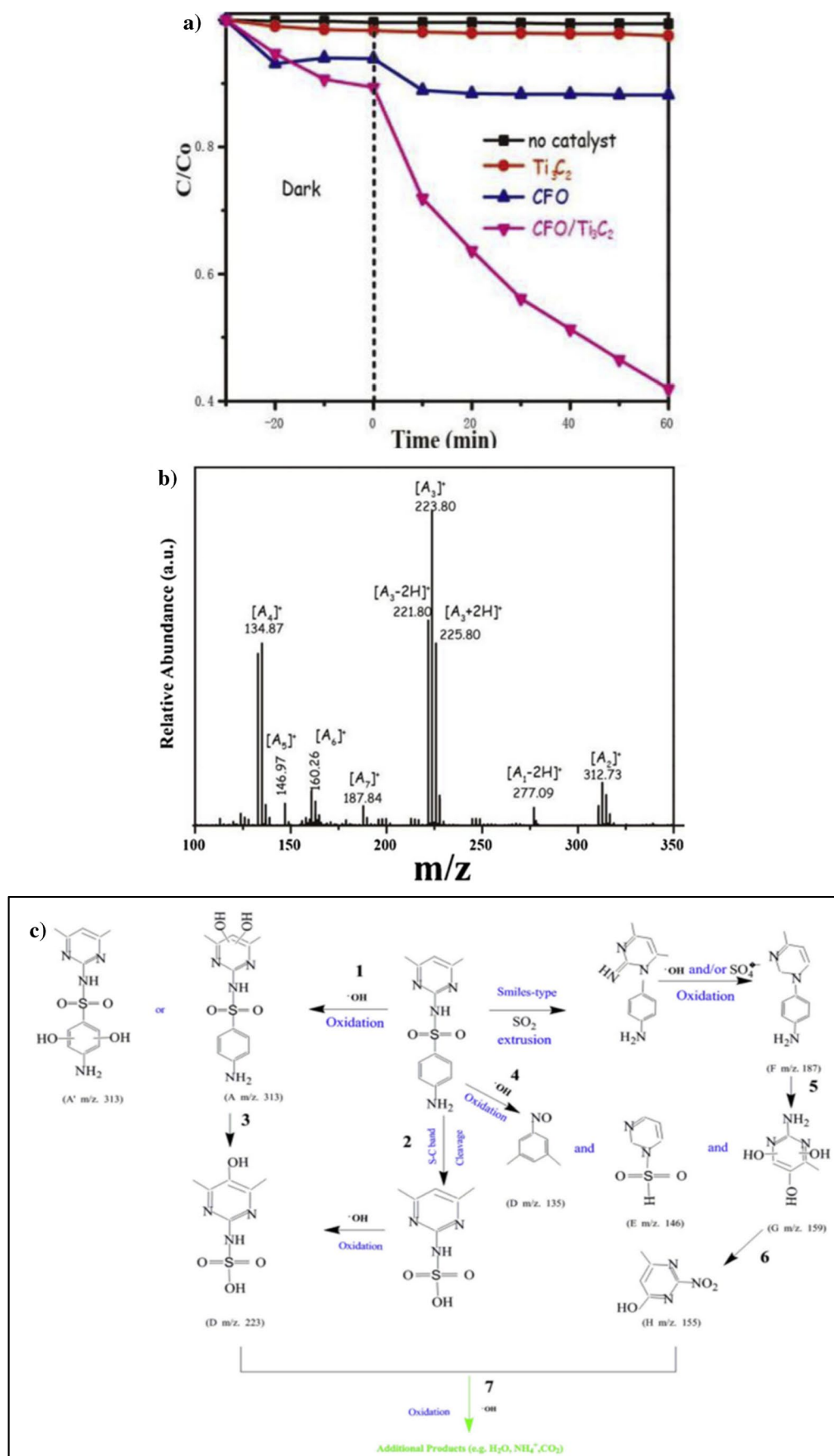ential applications, a lot of work has been done to use SC-based photocatalysts to degrade pollutants [188]. However, one of the major issues with most semiconductor photocatalysts was the charge recombination too quickly. The MXenes are the ideal alternative because they have a greater surface area, narrower bandgap energy, and the capacity to operate as electron acceptors, accelerating the separation of charges induced by the Schottky barrier. For instance, Ti_3C_2 and $TiSO_4$ were used as precursors in the hydrothermal method of TiO_2/Ti_3C_2 preparation by Gao et al. [189]. TiO_2 was also evenly dispersed, which increased the number of available active sites in the photodegradation process. A large number of active sites and high electrical conductivity lead to the effective degradation of MO than pure MXene.

Additionally, TiO_2/Ti_3C_2 ($TiO_2(1\ 1\ 1)/Ti_3C_2$) using the NH_4F-assisted hydrothermal oxidation procedure was reported by Chao et al. [190]. To upsurge the ratio of TiO_2, the NH_4F contents introduced throughout the fabrication was carefully regulated. According to the photodegradation data, increasing the exposed ratio upon the surface of titania optimized the MB dye degradation capability, mostly attributed to the much higher charge carrier efficiency. Additionally, the hydrazine hydrate treatment produced the -O vacancy, creating an excess of active sites for the photodegradation activity. Other semiconductors have been attached to the surface of Ti_3C_2 in addition to TiO_2 to enhance photocatalytic efficacy towards organic contaminants. CeO_2/Ti_3C_2 was created using an easy hydrothermal method by Zhou et al. [191], who also looked into the photocatalytic effectiveness of the material against RhB dye degradation. Researchers concluded that enhanced light utilization and enhanced charge carrier separation efficiency were responsible for CeO_2/Ti_3C_2's superior photocatalytic activity compared to pure Ti_3C_2 and CeO_2. Table 3 summarizes the results of photocatalytic degradation tests conducted on diverse pollutants using MXene-based composites.

In a different study, Cao et al. investigated the photocatalytic activities of $CuFe_2O_4/Ti_3C_2$ toward the breakdown of the antibiotic sulfamethazine [203]. Compared to pure

Table 3 MXene-based composites for degradation of inorganic and organic contaminants

Contaminant	Photocatalyst	Efficiency (in %)	References
Phenol, RhB, MB, and SCP	$CdS/Ti_3C_2/TiO_2$	100/150 min	[192]
Diclofenac	Magnetic-$Ti_3C_2T_x$	100/30 min	[193]
Ciprofloxacin	Ti_3C_2-Bi/BiOCl	89/100 min	[194]
RhB	$BiOBr/Ti_3C_2$	99.3/60 min	[195]
RhB	$NiCo_2S_4/Ti_3C_2T_x$	100/20 min	[196]
CR	Fe_3O_4/Ti_3C_2	98/14 min	[197]
MO	$In_2S_3/TiO_2@Ti_3C_2T_x$	95.8/60 min	[198]
RhB	$BiOBr/Ti_3C_2$	100/50 min	[199]
Tetracycline hydrochloride	Bi_2WO_6/Nb_2CT_x	83.1/90 min	[200]
RhB	$ZnO/Ti_3C_2T_x$	98/80 min	[201]
RhB	$g-C_3N_4/Ti_3C_2/TiO_2$	96.04/180 min	[202]

$CuFe_2O_4$ and Ti_3C_2, the produced $CuFe_2O_4/Ti_3C_2$ displayed a greater photocurrent density, indicating remarkable photogenerated charge carrier separation. As a result, the $CuFe_2O_4/Ti_3C_2$ combination outperformed pure $CuFe_2O_4$ and Ti_3C_2 regarding photocatalytic activity for the decomposition of sulfamethazine (Fig. 12a). Using liquid chromatography, as shown in Fig. 12b, to learn more about the sulfamethazine breakdown route. Characteristically, a peak at 277.09 was noted, attributed to sulfamethazine's dissociation. However, in addition to the peak described above, 7 more peaks were also observed at 134.87, 146.97, 155.46, 160.26, 187.84, 223.80, and 312.73. Based on these mass peaks, the photodegradation mechanism of sulfamethazine was hypothesized and shown in Fig. 12c. The hydroxyl ($^\bullet OH$) radicals then mineralized these mediators into CO_2, H_2O, and other molecules. Future research might benefit from this thorough investigation of the photodegradation route employing nanomaterials based on MXene.

According to Jiao et al. [204], post-treating MXene-based photocatalysts could be a very effective way to increase their photoactivity. They created a MoS_2/Ti_3C_2 nanocomposite using a hydrothermal technique, subjected it to friction treatment and assessed its photocatalytic activity for degrading MO dye. According to the findings, pure Ti_3C_2 and MoS_2 did not display the MoS_2/Ti_3C_2 nanocomposite has greatly improved photocatalytic activity. Rough surface leading to extra active sites for the photodegradation process was attributed to the improved photocatalytic activity. Ti_3C_2/Ag_2WO_4 nanocomposites were created by Fang et al. [205], and their adsorption and photocatalytic degradation effectiveness against sulfadimidine (SFE) and tetracycline hydrochloride were examined (TC). According to dark adsorption, Ag_2WO_4 and Ti_3C_2 appeared to have essentially nonexistent removal capacities against SFE and TC. However, the homogeneous integration of Ti_3C_2 improved the ability of Ag_2WO_4 to adsorb contaminants by reducing aggregation and decreasing surface adsorption of Ag_2WO_4. Ag_2WO_4/Ti_3C_2 demonstrated noticeably better photocatalytic activity against SFE and TC thanks to improved adsorption capacity and charged carrier separation efficiency. A 2D/2D Fe_2O_3/Ti_3C_2 magnetic nanocomposite was created by Zhang et al. [206] and used as a visible light active photocatalyst to degrade RhB dye. More than 90% of RhB dye can be removed in 60 min of visible light illumination, thanks to the discovery that $2D-Fe_2O_3$ might simply be introduced into the Ti_3C_2 layered structure to prevent agglomeration, resulting in enhanced charge carrier capability and increase in surface area. In addition to better charge carrier separation,

the increased surface area was a key factor in increased photocatalytic activity.

Making ternary composites is another useful strategy for increasing the degradation action of materials based on MXene for pollutant removal. A ternary $In_2S_3/TiO_2/Ti_3C_2$ composite was produced by Wang et al. [198] for the photodegradation of MO dye. EIS studies revealed that the $TiO_2/In_2S_3/Ti_3C_2$ nanocomposite was considerably more effective than pure In_2S_3 in removing photogenerated charge carriers. Type-2 heterojunction resulted in high removal efficacy leading to the enhanced transfer of electrons to holes. The TiO_2 surface's gathered electrons may also be transferred to those of Ti_3C_2. The photocatalytic activity data in Fig. 13a shows that the $In_2S_3/TiO_2/Ti_3C_2$ combination was more effective at photodegrading MO dye than the In_2S_3/CNT (58.4%), In_2S_3/rGO (19.7%), In_2S_3/TiO_2 (77.8%), and In_2S_3/MoS_2 (75.6%). The Z-scheme photocatalytic approach is among the best techniques to increase charge separation. The z-scheme consists of holes in the valence band and electrons in the conduction band, which provide higher oxidizing and reducing potential, respectively [192]. A $Ti_3C_2/TiO_2/CdS$ photocatalyst following the z-scheme by Liu et al. [192] was fabricated to investigate the functions. Photogenerated charge carrier separation efficiency was analyzed using the PL spectra (Fig. 13b). Their findings showed that the Z-scheme heterojunction development caused a decrease in PL intensity following CdS injection. Additionally, the produced compounds' photocatalytic effects on phenol, RhB, MB, and sulfachloropyridazine were investigated. According to the findings (Fig. 13c), MXene can act as a bridge for the transportation of charge carriers between semiconductor devices.

Scientists' attention has begun to grow on producing reusable magnetic photocatalysts. For the first instance, a magnetic MXene-based photocatalyst for RhB dye photodegradation was synthesized by Zhang et al. [207] and contained Ti_3C_2, $-Fe_2O_3$, and $ZnFe_2O_4$. Initially synthesized individually, the Ti_3C_2 and $-Fe_2O_3/ZnFe_2O_4$ were subsequently joined using an ultrasonic-assisted method. The photocatalytic findings indicate that $-Fe_2O_3/ZnFe_2O_4/Ti_3C_2$ had a benefit over $-Fe_2O_3/ZnFe_2O_4$ in terms of increased photocatalytic activity of $-Fe_2O_3/ZnFe_2O_4$, having a photocatalytic rate constant that was approximately three times higher. Additionally, the magnetic characteristics of $-Fe_2O_3$, $-ZnFe_2O_4$, and $-Ti_3C_2$ helped to separate them from the aqueous solution enabling simple recycling across four cycles.

4.3 EMI shielding

Because of its intriguing properties, MXene has been observed to act as a lightweight material for EMI shielding. These properties include solution processability, low density, outstanding metallic conductivity, tunable surface chemistry, large specific surface area, and superior shielding
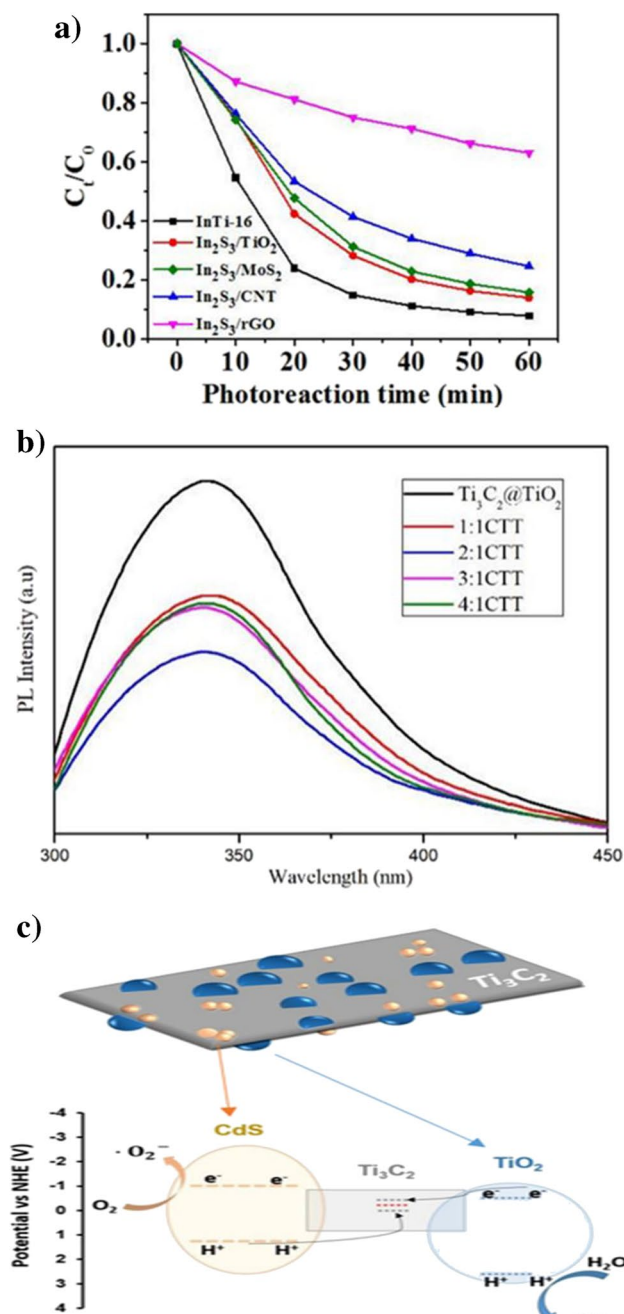
Fig. 13 a Time-dependent photocatalytic degradation of MO (reprinted with permission from [198] Elsevier, License No. 5435980910611), **b** PL spectra of pristine $Ti_3C_2@TiO_2$ along with 1 to 4% composite with CdS, **c** proposed degradation mechanism of $Ti_3C_2@TiO_2$ loaded with CdS [192]

performance. Therefore, several MXene composites and hybrids have been studied to advance the EMI shielding characteristics of MXenes. The innovation and rapid increase of electronic systems have grown quickly due to the downsizing of contemporary electronic circuits and equipment. Unfortunately, these tiny gadgets produce unwanted

EMI, which can impair the functionality of electrical systems [208]. Long-term exposure to electromagnetic (EM) radiation is bad for human health since it can lead to cancer, eye difficulties, nausea, headaches, and severe effects on the growth of a child's brain [209]. In addition, some surgical implants and equipment are prone to failure in a fluctuating electromagnetic field [210].

Due to the high EMI vulnerability of conventional combat, it is important to safeguard personnel and equipment against EM attack or contamination [211]. As a result, materials science has shifted its focus to figuring out how to stop or lessen the effects of hazardous electromagnetic radiation. Metals like copper, aluminum, Ag, and steel are broadly cast off to fight electromagnetic pollution because of their high conductivity [212]. Nevertheless, the use of MXene in highly combined contemporary portable electronics has been constrained by their high density, challenging processing ability, and high vulnerability to corrosion. For EMI shielding applications, a variety of heterogeneous composites with conducting fillers, such as 1D fillers, 2D fillers, magnetic fillers, and dielectric fillers. These composites have benefits like reduced weight, increased environmental resilience, and superior anticorrosive capabilities [213, 214]. Their poor shielding capacity, however, has restricted their application. There are a number of properties that make MXene an ideal EMI shielding material [43]. Because of their malleable surface chemistry, MXenes and composites may be fabricated into various forms. Due to the outstanding EMI shielding of 2D Ti3C2Tx, MXenes have quickly risen to the position of leading lightweight EMI shielding material, with a correspondingly increasing number of research papers [43].

Due to the mismatch in the air and shield impedance values, the shield interacts with the incoming em wave, and part of the wave gets reflected on the rear and front surfaces. Any residual power after attenuation or transmission is stored as heat in the shield (PT) [215]. The EMI SE is defined by Eq. (1) as the logarithmic ratio of the transmitted and incident powers and is used to characterize the degree to which a shield attenuates incident EM waves.

$$SE_T(dB) = 10 \log P_T/P_1 = 20 \log E_T/E_1 \tag{1}$$

where P and E represent the intensity of the electric field and the power of the electromagnetic waves that are incident and transmitted, respectively [36]. According to Schelkunoff's hypothesis, total EMI shielding effectiveness is represented by Eq. (2), which incorporates attenuation from reflection (SER), multiple reflection, and absorption [36].

$$SE_T = SE_R + SE_A + SE_M \tag{2}$$

It has been claimed that single metal $Ti_3C_2T_x$ ordered double metal $Mo_2TiC_2T_x$ and $Mo_2Ti_2C_3T_x$. Due to its greater electrical conductivity for $Mo_2TiC_2T_x$ and $Mo_2Ti_2C_3T_x$,

respectively, $Ti_3C_2T_x$ demonstrated the highest EMI shielding effectiveness. According to the reported literature, the electrical conductivity of $Ti_3C_2T_x$ MXene was several orders of magnitude greater than that of other conductive materials at the same thickness level. $Ti_3C_2T_x$ MXene was shown to be the most effective material for lightweight EMI shielding. EMI shielding mechanism by layered MXene structure has been proposed by schematic representation in Figure 14. Incoming EM waves are striking an MXene flake's surface. Because of the large number of charges on the highly conducting surface, some of the incident EM waves that travel through the MXene structure are instantly reflected off the surface. Local dipoles created by functionalized groups instead aid the absorption of incident waves. The same procedure is subsequently applied to waves that have less energy when they come into contact with another MXene flake, leading to numerous internal reflections as well as increased absorption. As a result, an EM wave's intensity significantly decreases each time it passes through an MXene flake, leading to an overall attenuated or entirely erased EM wave.

Due to its high electrical conductivity and laminate architecture, made feasible by the alignment of 2D flakes, $Ti_3C_2T_x$ MXene films provide exceptional EMI SE. After strongly interacting with the high electron density MXene layers in the layered structure of MXene, the residual EM waves are diminished by a combination of eddy current and ohmic losses. A subsequent study, where the Fresnel formula and attenuation rule presented theoretical calculations, provided more support for the good EMI shielding results of the $Ti_3C_2T_x$ MXene [216]. The theoretical calculations supported the experimental findings and highlighted $Ti_3C_2T_x$ MXene's exceptional potential as an EMI shielding material.

Ti_3C_2Tx MXene was synthesized using two alternative methods, and its EMI shielding abilities were assessed (as seen in Fig. 15). The M-$Ti_3C_2T_x$ composite included more F terminations than the U-$Ti_3C_2T_x$ composite's preponderance of O terminations. Ti_3C_2Tx MXenes were cold pressed at a pressure of 5 MPa after being mixed with an EM transparent SiO_2 nanoparticle matrix at varied mass ratios. U-Ti_3C_2Tx composite, with 60 wt% MXenes, has higher conductivity than M-Ti_3C_2Tx (6.3 105 S cm^{-1}). The 1-mm-thick 80 wt% U-Ti_3C_2Tx MXene composite has an EMI SE of 58 dB in the 8.2–12.4 GHz frequency band. U-Ti_3C_2Tx MXene composites fared better than M-Ti_3C_2Tx in EMI shielding because they had more conductive networks, greater surface area, and higher conductivity. Attenuation and dipolar polarization loss were further increased by the U-Ti_3C_2Tx MXene composite's larger exposed surface area, many surface terminations, and point defects.

MXene hybrids provide additional magnetic or conducting components to improve the shielding efficiency. The engagement between incident electromagnetic waves and the structure is enhanced by several phases, which can also increase mechanical qualities. For EMI shielding applications, thin, lightweight TiO_2-$Ti_3C_2T_x$/graphene hybrid laminate sheets have been produced [218]. Magnetic Ni chains and MXenes combine to produce outstanding EMI shielding performance. MXene laminates can be created at the

Fig. 14 Schematic of EMI shielding mechanism by layered MXene
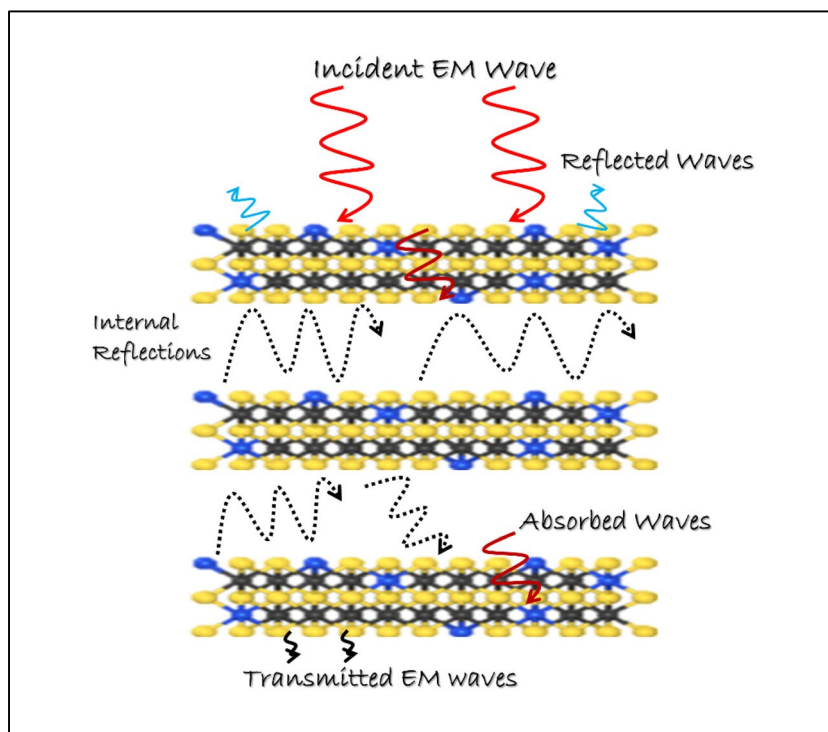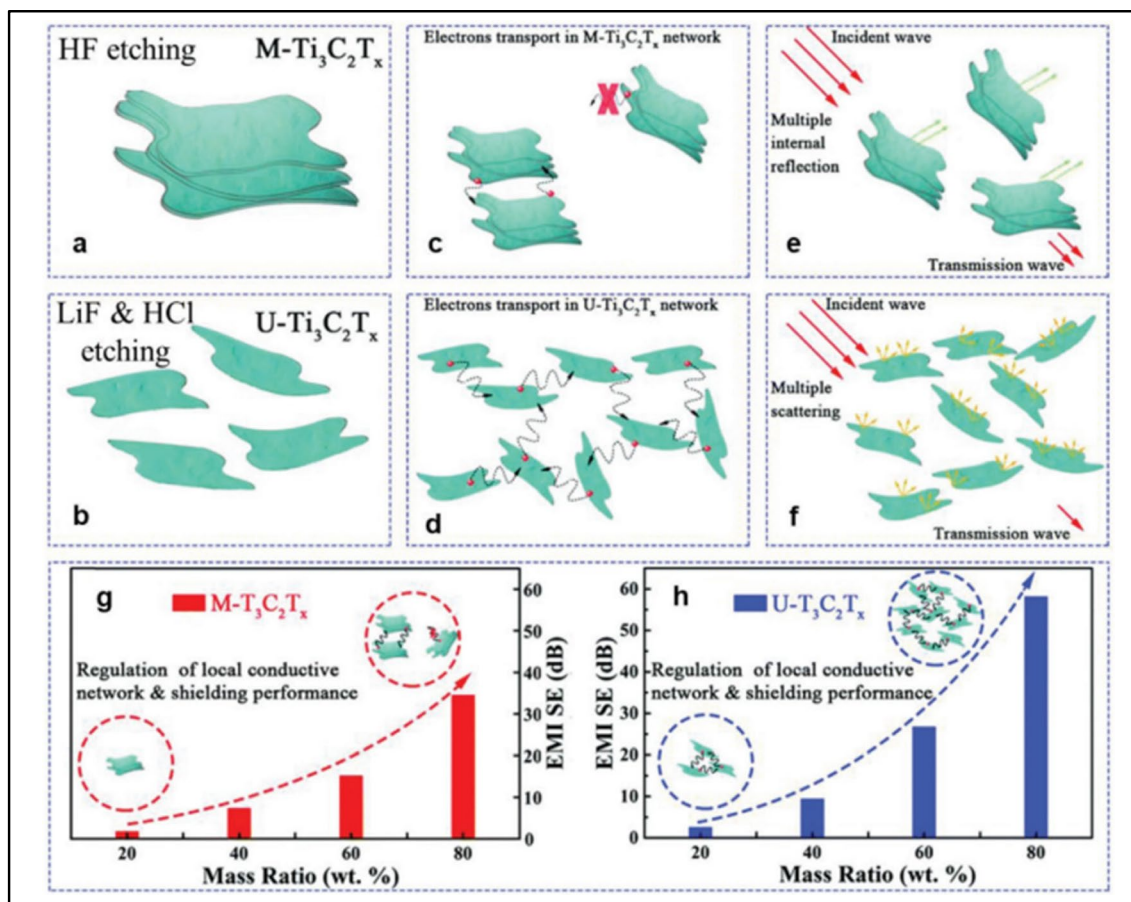
Fig. 15 Proposed EM interaction of Ti$_3$C$_2$T$_x$ composites [217]

nanoscale to fulfil the needs of commercial goods and offer superior EMI SE with a relatively low thickness. For aerospace and military applications, aerogels and porous foams provide effective, lightweight EMI shielding at the thickness loss. There is still much to learn about the new MXenes and their capacity to act as shields because the study of MXenes is still beginning.

4.4 HER

Because of the unique properties MXenes have, it has shown prodigious potential in hydrogen generation. Hydrogen has come to the forefront as a possible resolution to the global energy crisis and ecological dilapidation. Hydrogen has numerous advantages, including low greenhouse gas emissions and low pollution, a high energy density, and the ability to be recycled. In addition, due to its many positive characteristics, including little environmental impact, high reliability, low cost, and long lifespan, it may be easily integrated into green energy storage and conversion systems.

H$_2$ can be generated in many ways, including the combustion of fossil fuels, the fermentation of marsh gas, or the use of organic waste. In addition, an HER based on water splitting is beneficial economically and ecologically [219]. In order to produce hydrogen, the electrocatalyst is crucial, and costly metal-based electrocatalysts perform well. However, lack of resources and rising costs have made it difficult to meet the growing demand for electrocatalysts based on precious metals. It has therefore been a pressing task to continue developing high-efficient NPM-based HER electrocatalysts for producing hydrogen. Since then, a lot of advancements have been achieved, leading to the creation of the electrode materials phosphides, carbides, sulfides, nitrides, oxides, and nanocarbon free of metal particles [220–224]. However, two major issues remain the low electrical conductivity, which causes the active coating to thicken, and activity to drop rapidly. In addition, the issue is that these NPM-based materials do not exhibit adequate electrochemical reaction stability in aqueous solutions. MXenes are two-dimensional (2D) materials that mimic graphene and may offer solutions to the problems mentioned above.

The creation of hydrogen energy is an efficient response to the present energy and environmental concerns. Hydrogen evolution reaction (HER) is a vital method for creating

hydrogen and water splitting. It is crucial to develop HER catalysts with high stability, conductivity, and selectivity for use in the planned hydrogen economy. The high-performance electrocatalyst enables a reduced overpotential, increasing HER efficiency [225, 226]. Calculations using density functional theory (DFT) have shown that the Gibbs free energy of hydrogen adsorption (GH) is a good indication of HER activity [227]. When GH is most strongly linked to thermoneutrality, HER activity is at its highest. Compared to other NPM-based HER electrocatalysts, MXenes have a greater potential, and they also have other fantastic physical and chemical qualities: (a) MXenes rich in -OH and -O groups on their surface may form stable bonds with a variety of semiconductors. Because of their high electrical conductivity, MXenes (b) improve the efficiency of charge-carrier transfer. (c) MXenes may display more potent redox activity than carbon compounds due to the exposed metal sites at their terminals. (d) MXenes can contact water molecules appropriately thanks to their exceptional hydrophilicity. (e) The chemical and structural stability of MXenes in aqueous solutions is exceptional. In recent years, there has been a rise in theoretical and experimental study of HER electrocatalysts based on MXenes. Figure 16 shows how structural engineering has been used to enhance MXenes in hybridization, nanostructure creation, metal-atom doping, and termination modification. When compared to Pt-based catalysts, MXene-based materials show promise as electrocatalysts

Energy storage, conversion, and utilization rely on developing high-performance electrode materials and environmentally friendly NPM. Because of their remarkable hydrophilicity, strong metallic conductivity, and huge surface area, MXenes may be used in a variety of electrode applications
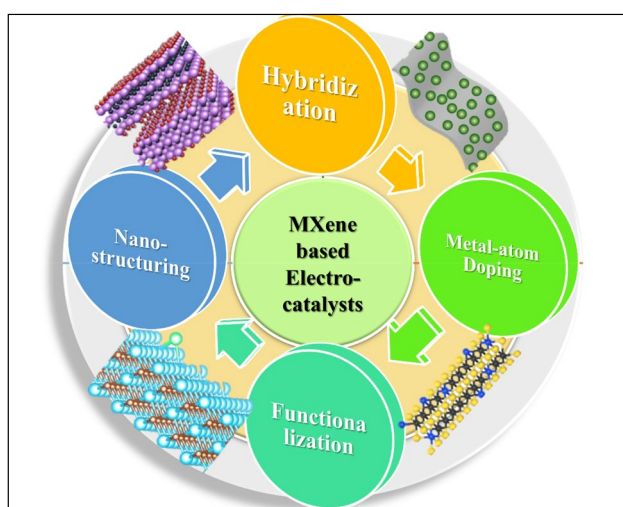
Fig. 16 Strategies for enhancing MXene-based HER electrocatalyst performance. Descriptive diagram summarizing numerous strategies for better results

[228]. Although substantial progress has been made over the last several decades in developing MXene-based electrocatalysts, there is still room for advancement if we are to build highly active, commercially viable electrocatalysts that are better than platinum-based materials. The surface functional groups of MXene are technique-dependent, and so remain a challenge to tune. This complexity of the surface environment has led to a continued debate about the catalytic process. Because of their limited yield, MXene nanostructures may be impractical for widespread use.

5 Summary and future prospective

Due to their unique properties, malleable structure, and component particles, MXenes are among the most inventive 2D materials developed for a wide range of applications. Adsorption, membrane filtration, and photocatalytic degradation of MXenes were intensively studied as potential applications in environmental cleanup. In order to make them more effective in wastewater treatment, recent studies have focused on improving their recyclable qualities, biocompatibility, and structural stability in both aqueous and ambient air environments. Surface chemistry, including selective oxidation and functionalization, may be precisely controlled to produce MXene analogues. Due to issues with long-term stability and aggregation in pure MXenes, a variety of polymeric MXene composites have been developed. If MXenes is to take the lead in environmental remediation, more research is needed to find solutions to the present problems. It is safe to say that MXenes are the materials of the future, having huge potential in fields like waste management and water purification.

While adsorption and catalytic degradation are two of the most common approaches to clean polluted water. The exciting discovery of extraordinary properties and performance of graphene-based nanomaterials, layered double hydroxides (LDHs), transition metal dichalcogenides, etc. have spurred a fast-developing interest in employing MXene-related materials for environmental applications. It is also shown that these materials have inherent challenges, such as the hydrophobicity of MoS_2, the expensive cost of graphene, and the low stability of LDHs under complex settings. Scholarly efforts have helped mitigate these difficulties, but resolving them remains challenging. MXenes and similar composites have established themselves in the literature as cutting-edge substance materials with significant promise in eliminating pollutants due to their superior performance. MXene-based materials are interesting for environmental applications because of their distinctive morphology, which includes properties such as changeable layer thickness, high hydrophilicity, adaptable structural design, a large specific surface area, and a wide compositional range. Among the numerous

new uses for MXene-based materials are the adsorption and catalytic degradation of various pollutants. These pollutants include oxidative metal ions, pigments, antibiotics, radioactive contaminants, organic compounds, heavy metal ions, and waste gases. Recently developed MXenes and MXene-based hybrids have been examined for their potential in environmental adsorption and catalytic degradation. The study of MXenes, in contrast to other two-dimensional materials, is in its infancy. Therefore, there are many open issues about their characteristics and their uses. At some point, conducting a thorough analysis of these concerns will be important. The technologies used for HF etching and the huge amounts of acidic gas and waste liquid produced during the preparation process must be improved. Even if a lot of time and energy has already been invested, there may be further avenues to explore. The search for more environmentally friendly preparation techniques continues. Research on the surface characteristics of MXene-based materials is sparse. Modifying MXene surfaces and doing more in-depth research into how surface properties affect MXene's stability in aqueous solution are two examples of what is needed to expand MXene's uses. Particularly for pollutant adsorption, surface engineering may significantly impact adsorption efficacy. Extensive research into MXenes in biological applications has led to early signs of their low toxicity; however, the toxicity and impacts of MXenes and their composites on the environment and people have not been well examined, nor are the toxicity mechanisms acknowledged. However, if these issues are addressed, MXenes will perform much better in environmental applications.

There have been considerable advances, but many obstacles remain, so developing high-performance MXene-based nanomaterials is urgent. Although there are now more ways to make MXene-supported semiconductor photocatalysts, many more are in the works. There are benefits and drawbacks to trying out novel synthetic approaches from scratch, such as having more say over product quality. The MXene family series may be expanded with the MXene family and vice versa. There are numerous conceivable heterogeneous structures between the structure of MXene and its photocatalytic performance, although many of its processes are still contested; MXene is quickly oxidized when kept for extended periods, making developing novel storage solutions vital; for instance, the efficiency of its electrical and photocatalytic systems will be impacted by quantum dot doping and surface modification. This issue has only been the focus of a few research studies in the last several years.

The high price of the photocatalytic MXene components employed in the preparation and the poor yield purity make it difficult to reach g-level mass manufacturing. This paves the way for further research on its preliminary theoretical foundations. Massive synthesis approaches are currently unrealistic. To prevent restacking, maintain a high surface area, and provide active attachment sites for target pollutants, the appropriate spacing between MXene-based layers must be changeable. This being the case, large-scale manufacturing of high-quality MXene of consistent size is essential for the future.

It is important to consider how MXene and nanomaterials made from it could affect our energy use and the natural world. Recent advances in MXene-based nanomaterials show promise in developing photocatalytic semiconductors, but there is still a long way to go before stable nanocatalysts can be created. Although MXene-based nanomaterials show much potential, they must undergo rigorous ecotoxicological testing and life-cycle analysis first. The kinetics and thermodynamic control technologies for MXene photocatalyst production need to be investigated in the future; MXene should be adjusted in tandem with theoretical analysis and experimental use. Theoretical calculations (density functional theory and basic principles) should be included in the catalyst design process to predict future structural performance, comprehend the whole MXene photocatalytic process, and perform a micro-level analysis of the mechanism.

Given its significant photocatalytic efficiency in removing water-borne organic pollutants, it is reasonable to expect that the MXene-based composite photocatalyst may also remove air pollutants (including volatile organic compounds, NO, SO_2, H_2S), NO_2, and other exhaust fumes. Despite MXene's promising photocatalytic performance, there is still an opportunity for advancement in integrating theory and experiment. There is an essential need to address the worldwide environmental crisis of air pollution. Few studies and publications address the potential of MXene-based composite photocatalysts for air purification; therefore, further research is needed. Researchers face new problems and opportunities as they explore MXene's vast potential across diverse sectors. We anticipate that our evaluation will contribute to the logical design of MXene-based materials, improving their efficiency and durability for real-world uses.

Availability of data and materials Data will be made available on request.

Declarations

Ethics approval Not applicable.

Conflict of interest The authors declare no competing interests.

Refe rences

1. S.A. Bahadi, M. Iddrisu, M.K. Al-Sakkaf, M.A.A. Elgzoly, W.A. Al-Amrani, U. Ahmed, Q.A. Drmosh, S.A. Ohaizi, Chemically versus thermally reduced graphene oxide: effect of reduction methods and reducing agents on the adsorption of phenolic compounds from waster water. Emergent Mater. (2023)

2. M.L. Malati, A. Abrahams, V. Chauke, L.N. Dlamini, Rhus vernicifera laccase immobilization on Ti2N MXene as a potential biocatalyst in environmental remediation. Emergent Mater. **6**, 245–260 (2023)

3. N. Lele, M.F. Bambo, E.M. Mmutlane, L.N. Dlamini, Construction of a multifunctional MXene @ β-cyclodextrin nanocomposite with photocatalytic properties. Emergent Mater. **6**, 605–626 (2023)

4. M. Vijaykumar, G. Elsa, A. Nirogi, R. Navaneethan, A.B. Sankar, M. Kathik, MXenes and their composites for hybrid capacitors and supercapacitors: a critical review. Emergent Mater. **4**, 655–672 (2021)

5. J.S. George, A. Uthaman, A. Reghunadhan, H.M. Lal, S. Thomas, P. Vijayan, Bioderived thermosetting polymers and their nanocomposites: current trends and future outlook. Emergent Mater. **5**, 3–27 (2022)

6. M.D.M. Islam, D.M. Ahmad, H. Shahariar, An approach to develop electrically conductive cotton yarn by facile multilayered deposition of silver particles. Emergent Mater. **6**, 1027–1036 (2023)

7. B.R. Babu, B. Rao, Electromagnetic interference shielding behaviour of stacked aloe vera and silk fibre-reinforced high-content copper slag power epoxy sandwich composite. Emergent Mater. **6**, 1363–1370 (2023)

8. A.K. Geim, I.V.J.N. Grigorieva, Van der Waals heterostructures. Nature **499**(7459), 419–425 (2013)

9. S. Sardana, Z. Singh, A.K. Sharma, N. Kaur, P.K. Pati, A. Mahajan, Self powered biocompatible humidity sensor based on an electrospun anisotropic triboelectric nanogenerator for non invasive diagnostic applications. Sens. Actuators B **537**, 132507 (2022)

10. S. Sardana, H. Kaur, B. Arora, D.K. Aswal, A. Mahajan, Self powered monitoring of ammonia using an MXene/TiO2/cellulose nanofibre heterojunction-based sensor driven by an electrospun triboelectric nanogenerator. ACS Sensors **7**, 312–321 (2022)

11. V. Sharma, R. Dhiman, A. Mahajan, Ti2+ and Ti4+ species enriched MXene electrocatalysts for highly hydrogen evolution and oxygen evolution reaction kinetics. Appl. Surf. Sci. **612**, 155883 (2023)

12. M. Naguib et al., Two-dimensional nanocrystals produced by exfoliation of Ti3AlC2. Adv. Mater. **23**, 4248–4253 (2011)

13. B. Anasori, M..R. Lukatskaya, Y.J.N.R.M. Gogotsi, 2D metal carbides and nitrides (MXenes) for energy storage. Nat. Rev. Mater **2**, 1–17 (2017)

14. B. Anasori et al., Two-dimensional, ordered, double transition metals carbides (MXenes). ACS Nano. **9**(10), 9507–9516 (2015)

15. A. Petruhins, J. Lu, L. Hultman, J.J.M.R.L. Rosen, Rosen, Synthesis of atomically layered and chemically ordered rare-earth (RE) i-MAX phases; (Mo2/3RE1/3) 2GaC with RE= Gd, Tb, Dy, Ho, Er, Tm, Yb, and Lu. Res. Lett. **7**(11), 446–452 (2019)

16. M. Dahlqvist, J. Lu, R. Meshkian, Q. Tao, L. Hultman, J. Rosen, Prediction and synthesis of a family of atomic laminate phases with Kagomé-like and in-plane chemical ordering. Science. **3**(7), e1700642 (2017)

17. M. Dahlqvist, A. Petruhins, J. Lu, L. Hultman, J. Rosen, Origin of chemically ordered atomic laminates (i-MAX): expanding the elemental space by a theoretical/experimental approach. ACS Nano. **12**(8), 7761–7770 (2018)

18. A.C. Rajan et al., Machine-learning-assisted accurate band gap predictions of functionalized MXene. Chem. Mater. **30**(12), 4031–4038 (2018)

19. W.-T. Wang et al., When MOFs meet MXenes: superior ORR performance in both alkaline and acidic solutions. J. Mater. Chem. A. **9**(7), 3952–3960 (2021)

20. S. Uppugalla, R. Pothu, R. Boddula, M.A. Deasai, N. Al-Qahtani, Nitrogen and sulfur co-doped activated carbon nanosheets for high performance coin cell supercapacitor device with outstanding cycle stability. Emergent Mater **6**, 1167–1176 (2023)

21. S. Anwer et al., 2D Ti3C2Tx MXene nanosheets coated cellulose fibers based 3D nanostructures for efficient water desalination. Chem. Eng. J. **406**, 126827 (2021)

22. W. Huang, L. Hu, Y. Tang, Z. Xie, H.J.A.F.M. Zhang, Recent advances in functional 2D Mxene-based nanostructures for next-generation devices. Adv. Funct. Mater. **30**(49), 2005223 (2020)

23. H. Kim, H.N.J.A.M. Alshareef, MXetronics: MXene-enabled electronic and photonic devices. ACS Materials Lett **2**(1), 55–70 (2019)

24. F. Shahzad, A. Iqbal, H. Kim, C.M.J.A.M. Koo, 2D transition metal carbides (MXenes): applications as an electrically conducting material. Adv. Mater. **32**(51), 2002159 (2020)

25. Z. Xie et al., Solar-inspired water purification based on emerging 2D materials: status and challenges. Sol. RRL. **4**(3), 1900400 (2020)

26. S. Archana, D. Radhika, B. Jayanna, K. Kannan, K.Y. Kumar, H.J.F. Muralidhara, Functionalization and partial grafting of the reduced graphene oxide with p-phenylenediamine: an adsorption and photodegradation studies. FlatChem. **26**, 100210 (2021)

27. S. Kim et al., Enhanced adsorption performance for selected pharmaceutical compounds by sonicated Ti3C2Tx MXene. Chem. Eng. J. **406**, 126789 (2021)

28. C.E. Ren, K.B. Hatzell, M. Alhabeb, Z. Ling, K.A. Mahmoud, Y. Gogotsi, Charge- and size-selective ion sieving through Ti3C2Tx MXene membranes. J. Phys. Chem. Lett. **6**, 4026–4031 (2015)

29. Z. Xie et al., The rise of 2D photothermal materials beyond graphene for clean water production. Adv. Sci. **7**, 1902236 (2020)

30. S.-M. Lam et al., Surface decorated coral-like magnetic BiFeO3 with Au nanoparticles for effective sunlight photodegradation of 2,4-D and E. coli inactivation. J. Mol. Liq. **326**, 115372 (2021)

31. Y. Gogotsi, Q.J. Huang, *MXenes: two-dimensional building blocks for future materials and devices*, vol 15 (ACS Publications, 2021), pp. 5775–5780

32. Z. Xiu et al., Recent advances in Ti3+ self-doped nanostructured TiO2 visible light photocatalysts for environmental and energy applications. Chem. Eng. J. **382**, 123011 (2020)

33. C. Prasad, H. Tang, Q. Liu, I. Bahadur, S. Karlapudi, Y. Jiang, A latest overview on photocatalytic application of g-C3N4 based nanostructured materials for hydrogen production. Int. J. Hydrogen Energy **45**, 337–379 (2020)

34. S. Yang et al., Fluoride-free synthesis of two-dimensional titanium carbide (MXene) using a binary aqueous system. Angew. Chem. **130**, 15717–15721 (2018)

35. X.-F. Yu et al., Monolayer Ti2CO2: a promising candidate for NH3 sensor or capturer with high sensitivity and selectivity. ACS Appl. Mater. Interfaces **7**, 13707–13713 (2015)

36. B. Anasori, Y. Gogotsi, in *2D Metal carbides and nitrides (MXenes)*. Introduction to 2D transition metal carbides and nitrides (MXenes) (Springer, 2019), pp. 3–12

37. X. Zheng et al., Multifunctional RGO/Ti3C2Tx MXene fabrics for electrochemical energy storage, electromagnetic interference shielding, electrothermal and human motion detection. Mater. Des **200**, 109442 (2021)

38. L. Xu et al., In-situ anchoring of Fe3O4/ZIF-67 dodecahedrons in highly compressible wood aerogel with excellent microwave absorption properties. Mater. Des **182**, 108006 (2019)

39. K.M. Batoo, M. Hadi, R. Verma, A. Chauhan, R. Kumar, M. Singh, O.M. Aldossary, Improved microwave absorption and EMI shielding properties of Ba-doped Co-Zn ferrite. Ceram. Int. **48**, 3328–3343 (2022)

40. K.M. Batoo, M. Hadi, A. Chauhan, R. Verma, M. Singh, O.M. Aldossary, G.K. Bhargawa, High frequency applications of bismuth-doped Co-Zn ferrite nanoparticles for electromagnetic interference filter and multilayer inductor chip fabrication. Appl. Phys. A **128**, 283 (2022)

41. D. Hu, X. Huang, S. Li, P. Jiang, Flexible and durable cellulose/MXene nanocomposite paper for efficient electromagnetic interference shielding. Compos. Sci.Technol. **188**, 107995 (2020)

42. R. Verma, P. Thakur, A. Chauhan, R. Jasrotia, A. Thakur, A review on MXene and its composite for electromagnetic interference (EMI) shielding applications. Carbon **208**, 170–190 (2023)

43. Y. Zhang et al., Adsorptive environmental application of MXene nanomaterials: a review. RSC Adv. **8**, 19895–19905 (2018)

44. B.-M. Jun et al., Review of MXenes as new nanomaterials for energy storage/delivery and selected environmental application. Nano Res. **12**, 471–487 (2019)

45. Y. Sun, Y. Li, Potential environmental applications of MXenes: a critical review. Chemosphere **271**, 129578 (2021)

46. Chen et al., Recent progress in environmental remediation, colloidal behavior and biological effects of MXene: a review. Environ. Sci. Nano. **9**, 3168–3205 (2022)

47. S. Saxena, M. Johnson, F. Dixit, K. Zinnermann, S. Chaudhuri, K. Kaka, B. Kandasubramanian, Thinking green with 2-D and 3-D MXenes: environment friendly synthesis and industrial scale applications and global impact. Renew. Sustain. Energy Rev. **178**, 113238 (2023)

48. H. Chaudhuri, Y.S. Yun, A critical review on the properties and energy storage applications of graphene oxide/layered double hydroxides and graphene oxide/ MXenes. J. Power Sources **564**, 232870 (2023)

49. F.A. Janjhi, I. Sahanullah, M. Bilal, R.C. Munoz, G. Boczkaj, F. Gallucci, MXene-based materials for removal of antibiotics and heavy metals from waste water-a review. Water Res. Ind. **29**, 100202 (2023)

50. B. Anasori, M. Naguib, Two dimensional MXenes. MRS Bull. **48**, 238–244 (2023)

51. A.S. Jatoi, N.M. Mubarak, Z. Hashmi, N.H. Solangi, R.R. Karri, Y.H. Tan, S.A. Mazari, J.R. Koduru, A. Alfantazi, New insights into MXene applications for sustainable environmental remediation. Chemosphere **313**, 137497 (2023)

52. I. Raheem, N.M. Mubarak, R.R. Karri, N.H. Solangi, A.S. Jatoi, S.A. Mazari, M. Khalid, Y.H. Tan, J.R. Koduru, G. Malafaia, Rapid growth of MXene based membranes for sustainable environmental pollution remediation. Chemosphere **311**, 137056 (2023)

53. Q. Wang, N. Han, Z. Shen, X. Li, Z. Chen, Y. Cao, W. Si, F. Wang, B. Ni, V.K. Thakur, MXene-based electrochemical (bio) sensors for sustainable applications: roadmap for future advanced materials. Nano Mater. Sci. **5**, 39–52 (2023)

54. F. Dixit, K. Zimmermann, M. ALmoudi, L. Abkar, B. Barbeau, M. Mohseni, B. Kandasubramanian, K. Smith, Application of MXenes for air purification, gas separation and storage: a review. Renew. Sustain. Energy Rev. **164**, 112527 (2022)

55. Q. Tao et al., Two-dimensional Mo1.33C MXene with divacancy ordering prepared from parent 3D laminate with in-plane chemical ordering. Nat. Commun. **8**, 14449 (2017)

56. M.D. Firouzhaei, S.K. Nemani, M. Sadrzadeh, E.K. Wujcik, M. Elliott, B. Anasori, Life cycle assessment of Ti3C2Tx MXene synthesis. Adv. Mater. **35**, 2300422 (2023)

57. M. Chang, Q. Li, Z. Jia, W. Zhao, G. Wu, Tuning microwave absorption properties of Ti3C2Tx MXene-based materials: component optimization and structure modulation. J. Mater. Sci. Technol. **148**, 150–170 (2023)

58. M.A. Hope et al., NMR reveals the surface functionalisation of Ti3C2 MXene. Phys. Chem. Chem. Phys. **18**, 5099–5102 (2016)

59. X. Xie, N. Zhang, Positioning MXenes in the photocatalysis landscape: competitiveness, challenges, and future perspectives. Adv. Funct. Mater. **30**, 2002528 (2020)

60. M. Alhabeb et al., Guidelines for synthesis and processing of two-dimensional titanium carbide (Ti3C2T x MXene). Chem. Mater. **29**, 7633–7644 (2017)

61. M. Naguib, V.N. Mochalin, M.W. Barsoum, Y. Gogotsi, 25th anniversary article: MXenes: a new family of two-dimensional materials. Adv. Mater. **26**, 992–1005 (2014)

62. M. Naguib et al., Two-dimensional nanocrystals produced by exfoliation of Ti3 AlC2. Adv. Mater. **23**, 4248–4253 (2011)

63. J. Halim et al., Transparent conductive two-dimensional titanium carbide epitaxial thin films. Chem. Mater. **26**, 2374–2381 (2014)

64. M. Ghidiu, M.R. Lukatskaya, M.-Q. Zhao, Y. Gogotsi, M.W. Barsoum, Conductive two-dimensional titanium carbide 'clay' with high volumetric capacitance. Nature **516**, 78–81 (2014)

65. M. Naguib, R.R. Unocic, B.L. Armstrong, J. Nanda, Large-scale delamination of multi-layers transition metal carbides and carbonitrides "MXenes". Dalton Trans. **44**, 9353–9358 (2015)

66. A. Feng et al., Two-dimensional MXene Ti3C2 produced by exfoliation of Ti3AlC2. Mater. Des **114**, 161–166 (2017)

67. M.A. Hejazi, O. Eksik, C.T. Yucedag, C. Unlu, L. Trabzon, Carbon based nanomaterials in gas sensing application. Emergent Mater. **6**, 45–77 (2023)

68. N. Zhang, Y. Hong, S. Yazdanparast, M. Asle Zaeem, Superior structural, elastic and electronic properties of 2D titanium nitride MXenes over carbide MXenes: a comprehensive first principles study. 2D Materials **5**, 045004 (2018)

69. P. Urbankowski et al., Synthesis of two-dimensional titanium nitride Ti4N3 (MXene). Nanoscale **8**, 11385–11391 (2016)

70. B. Soundiraraju, B.K. George, Two-dimensional titanium nitride (Ti2N) MXene: synthesis, characterization, and potential application as surface-enhanced Raman scattering substrate. ACS Nano **11**, 8892–8900 (2017)

71. X. Zhang et al., Novel solvothermal preparation and enhanced microwave absorption properties of Ti3C2Tx MXene modified by in situ coated Fe3O4 nanoparticles. Appl. Surf. Sci. **484**, 383–391 (2019)

72. S. Venkateshalu et al., New method for the synthesis of 2D vanadium nitride (MXene) and its application as a supercapacitor electrode. ACS Omega **5**, 17983–17992 (2020)

73. F. Shahzad et al., Electromagnetic interference shielding with 2D transition metal carbides (MXenes). Science (New York, NY) **353**(6304), 1137–1140 (2016). https://doi.org/10.1126/science.aag2421

74. O.C. Francis, A.V. Sunday, Highly enhanced mechanical, electrical and thermal properties of carbon nanotubes/biologically produced silver nanoparticles/epoxy composites. Emergent Mater. **6**, 89–99 (2023)

75. B. Konerui, P. Banerjee, A. Franco Jr., Controlled defects and trap-assisted mitigation in Li-intercalated zinc oxide ceramics. Emergent Mater. **6**, 315–320 (2023)

76. T. Li et al., Fluorine-free Ti$_3$C$_2$T$_x$ (T = O, OH) nanosheets (~50–100 nm) for nitrogen fixation under ambient conditions. J. Mater. Chem. A **7**, 14465 (2019)

77. X. Yu, X. Cai, H. Cui, S.-W. Lee, X.-F. Yu, B. Liu, Fluorine-free preparation of titanium carbide MXene quantum dots with high near-infrared photothermal performances for cancer therapy. Nanoscale **9**, 17859–17864 (2017)

78. J. Xuan et al., Organic-base-driven intercalation and delamination for the production of functionalized titanium carbide nanosheets with superior photothermal therapeutic performance. Angew. Chem. Int. Ed. Engl. **55**, 14569–14574 (2016)

79. N. Xue, X. Li, M. Zhang, L. Han, Y. Liu, X. Tao, Chemical-combined ball-milling synthesis of fluorine-free porous MXene for high-performance lithium ion batteries. ACS Appl. Energy Mater. **3**, 10234–10241 (2020)

80. M. Song, S.Y. Pang, F. Guo, M.C. Wong, J. Hao, Fluoride-free 2D niobium carbide MXenes as stable and biocompatible nanoplatforms for electrochemical biosensors with ultrahigh sensitivity. Adv. Sci. **7**, 2001546 (2020)

81. S.-Y. Pang et al., Universal strategy for HF-free facile and rapid synthesis of two-dimensional MXenes as multifunctional energy materials. J. Am. Chem. Soc. **141**, 9610–9616 (2019)

82. S.Y. Pang, W.F. Io, L.W. Wong, J. Zhao, J. Hao, Efficient energy conversion and storage based on robust fluoride-free self-assembled 1D niobium carbide in 3D nanowire network. Adv. Sci. **7**, 1903680 (2020)

83. Z. Sun et al., Selective lithiation–expansion–microexplosion synthesis of two-dimensional fluoride-free Mxene. ACS Mater. Lett. **1**, 628–632 (2019)

84. Y. Li et al., Author correction: a general Lewis acidic etching route for preparing MXenes with enhanced electrochemical performance in non-aqueous electrolyte. Nat. Mater. **20**, 571 (2021)

85. Y. Gogotsi, Chemical vapour deposition: transition metal carbides go 2D. Nat. Mater. **14**, 1079–1080 (2015)

86. C. Xu et al., Large-area high-quality 2D ultrathin Mo2C superconducting crystals. Nat. Mater. **14**, 1135–1141 (2015)

87. M. Alhabeb et al., Guidelines for synthesis and processing of two-dimensional titanium carbide (Ti3C2Tx MXene). Chem. Mater. **29**, 7633–7644 (2017)

88. Y. Gogotsi, Transition metal carbides go 2D. Nat. Mater. **14**, 1079–1080 (2015)

89. D. Geng et al., Direct synthesis of large-area 2D Mo(2) C on in situ grown graphene. Adv. Mater. **29**, 1700072 (2017)

90. L. Gao et al., MXene/polymer membranes: synthesis, properties, and emerging applications. Chem. Mater. **32**, 1703–1747 (2020)

91. A. Lipatov et al., High electrical conductivity and breakdown current density of individual monolayer Ti3C2Tx MXene flakes. Matter **4**, 1413–1427 (2021)

92. S. Joshi, Q. Wang, A. Puntambekar, V. Chakrapani, Facile synthesis of large area two-dimensional layers of transition-metal nitride and their use as insertion electrodes. ACS Energy Lett. **2**, 1257–1262 (2017)

93. O. Mashtalir, M.R. Lukatskaya, M.Q. Zhao, M.W. Barsoum, Y. Gogotsi, Amine-assisted delamination of Nb2C MXene for Li-ion energy storage devices. Adv. Mater. **27**, 3501–3506 (2015)

94. O. Mashtalir et al., Intercalation and delamination of layered carbides and carbonitrides. Nat. Commun. **4**, 1716 (2013)

95. R. Ma, T. Sasaki, Two-dimensional oxide and hydroxide nanosheets: controllable high-quality exfoliation, molecular assembly, and exploration of functionality. Acc. Chem. Res. **48**, 136–143 (2015)

96. N. Uetake, F. Kawamura, H. Yusa, Alternative solvent wash process using tetramethylammonium hydroxide solution as salt-free wash reagent. J. Nucl. Sci. Technol. **26**, 270–277 (1989)

97. W.K. Musker, A reinvestigation of the pyrolysis of tetramethylammonium hydroxide. J. Am. Chem. Soc. **86**, 960–961 (1964)

98. Y.-W. Cheng, J.-H. Dai, Y.-M. Zhang, Y. Song, Two-dimensional, ordered, double transition metal carbides (MXenes): a new family of promising catalysts for the hydrogen evolution reaction. J. Phys. Chem. C **122**, 28113–28122 (2018)

99. L.H. Karlsson, J. Birch, J. Halim, M.W. Barsoum, P.O. Persson, Atomically resolved structural and chemical investigation of single MXene sheets. Nano Lett. **15**, 4955–4960 (2015)

100. I. Persson et al., Tailoring structure, composition, and energy storage properties of MXenes from selective etching of in-plane, chemically ordered MAX phases. Small **14**, 1703676 (2018)

101. Q. Tao et al., Two-dimensional Mo(1.33)C MXene with divacancy ordering prepared from parent 3D laminate with in-plane chemical ordering. Nat. Commun. **8**, 14949 (2017)

102. J. Halim et al., Synthesis of two-dimensional Nb1.33C (MXene) with randomly distributed vacancies by etching of the quaternary solid solution (Nb2/3Sc1/3)2AlC MAX Phase. ACS Appl. Nano Mater. **1**, 2455–2460 (2018)

103. N.C. Osti et al., Effect of metal ion intercalation on the structure of MXene and water dynamics on its internal surfaces. ACS Appl. Mater. Interfaces **8**, 8859–8863 (2016)

104. C.J. Zhang et al., Oxidation stability of colloidal two-dimensional titanium carbides (MXenes). Chem. Mater. **29**, 4848–4856 (2017)

105. J. Pang et al., Applications of 2D MXenes in energy conversion and storage systems. Chem. Soc. Rev. **48**, 72–133 (2019)

106. L. Wang, W. Liu, Z. He, Z. Guo, A. Zhou, A. Wang, Cathodic hydrogen recovery and methane conversion using Pt coating 3D nickel foam instead of Pt-carbon cloth in microbial electrolysis cells. Int. J. Hydrog. Energy **42**, 19604–19610 (2017)

107. L. Li, Lattice dynamics and electronic structures of Ti3C2O2 and Mo2TiC2O2 (MXenes): the effect of Mo substitution. Comput. Mater. Sci. **124**, 8–14 (2016)

108. R.M. Ronchi, J.T. Arantes, S.F. Santos, Synthesis, structure, properties and applications of MXenes: current status and perspectives. Ceram. Int. **45**, 18167–18188 (2019)

109. X. Wang et al., A new etching environment (FeF$_3$/HCl) for the synthesis of two-dimensional titanium carbide MXenes: a route towards selective reactivity vs. water. J. Mater. Chem. A **5**, 22012–22023 (2017)

110. K. Hantanasirisakul, Y. Gogotsi, Electronic and optical properties of 2D transition metal carbides and nitrides (MXenes). Adv. Mater. **30**, 1804779 (2018)

111. A.V. Mohammadi, J. Rosen, Y. Gogotsi, The world of two-dimensional carbides and nitrides (MXenes). Science **372**, eabf1581 (2021)

112. K. Wang, Y. Zhou, W. Xu, D. Huang, Z. Wang, M. Hong, Fabrication and thermal stability of two-dimensional carbide Ti3C2 nanosheets. Ceram. Int. **42**, 8419–8424 (2016)

113. S. Li et al., Ultrathin MXene nanosheets with rich fluorine termination groups realizing efficient electrocatalytic hydrogen evolution. Nano Energy **47**, 512–518 (2018)

114. I. Persson et al., 2D transition metal carbides (MXenes) for carbon capture. Adv. Mater. **31**, 1805472 (2019)

115. Z. Li et al., Synthesis and thermal stability of two-dimensional carbide MXene Ti3C2. Mater. Sci. Eng.: B **191**, 33–40 (2015)

116. H. Kim, B. Anasori, Y. Gogotsi, H.N. Alshareef, Thermoelectric properties of two-dimensional molybdenum-based MXenes. Chem. Mater. **29**, 6472–6479 (2017)

117. J. Zhou et al., A two-dimensional zirconium carbide by selective etching of Al3C3 from nanolaminated Zr3Al3C5. Angew. Chem. Int. Ed. **55**, 5008–5013 (2016)

118. A. Feng et al., Fabrication and thermal stability of NH4HF2-etched Ti3C2 MXene. Ceram. Int. **43**, 6322–6328 (2017)

119. Y. Bai, K. Zhou, N. Srikanth, J.H.L. Pang, X. He, R. Wang, Dependence of elastic and optical properties on surface

terminated groups in two-dimensional MXene monolayers: a first-principles study. RSC Adv. **6**, 35731–35739 (2016)

120. X.-H. Zha et al., Role of the surface effect on the structural, electronic and mechanical properties of the carbide MXenes. Europhys. Lett. **111**, 26007 (2015)

121. Z. Guo, J. Zhou, C. Si, Z. Sun, Flexible two-dimensional Ti n+1 C n (n= 1, 2 and 3) and their functionalized MXenes predicted by density functional theories. Phys. Chem. Chem. Phys. **17**, 15348–15354 (2015)

122. V.N. Borysiuk, V.N. Mochalin, Y. Gogotsi, Molecular dynamic study of the mechanical properties of two-dimensional titanium carbides Tin^{+1}Cn (MXenes). Nanotechnology **26**, 265705 (2015)

123. U. Yorulmaz, A. Özden, N.K. Perkgöz, F. Ay, C. Sevik, Vibrational and mechanical properties of single layer MXene structures: a first-principles investigation. Nanotechnology **27**, 335702 (2016)

124. M. Naguib et al., Ti3C2Tx (MXene)–polyacrylamide nanocomposite films. RSC Adv. **6**, 72069–72073 (2016)

125. E.A. Mayerberger, O. Urbanek, R.M. McDaniel, R.M. Street, M.W. Barsoum, C.L. Schauer, Preparation and characterization of polymer-Ti3C2Tx (MXene) composite nanofibers produced via electrospinning. J. Appl. Polym. Sci. **134**, 45295 (2017)

126. H. Zhang et al., Preparation, mechanical and anti-friction performance of MXene/polymer composites. Materials & Design **92**, 682–689 (2015)

127. M. Khazaei, A. Ranjbar, M. Arai, S. Yunoki, Topological insulators in the ordered double transition metals M₂′M″C₂ MXenes (M′= Mo, W; M ″= Ti, Zr, Hf). Physical Review B **94**, 125152 (2016)

128. K. Hantanasirisakul et al., Fabrication of Ti3C2Tx MXene transparent thin films with tunable optoelectronic properties. Adv. Electron. Mater. **2**, 1600050 (2016)

129. Y. Liu, H. Xiao, W.A. Goddard, Schottky-barrier-free contacts with two-dimensional semiconductors by surface-engineered MXenes. J. Am. Chem. Soc. **138**, 15853–15856 (2016)

130. L.-F. Hong et al., Recent progress of two-dimensional MXenes in photocatalytic applications: a review. Mater. Today Energy **18**, 100521 (2020)

131. X. Zhan, C. Si, J. Zhou, Z. Sun, MXene and MXene-based composites: synthesis, properties and environment-related applications. Nanoscale Horiz. **5**, 235–258 (2020)

132. Q. Tang, Z. Zhou, P. Shen, Are MXenes promising anode materials for Li ion batteries? Computational studies on electronic properties and Li storage capability of Ti3C2 and Ti3C2X2 (X = F, OH) monolayer. J. Am. Chem. Soc. **134**, 16909–16916 (2012)

133. Q. Meng et al., Theoretical investigation of zirconium carbide MXenes as prospective high capacity anode materials for Na-ion batteries. J. Mater. Chem. A **6**, 13652–13660 (2018)

134. F. Wu et al., Theoretical understanding of magnetic and electronic structures of Ti3C2 monolayer and its derivatives. Solid State Commun. **222**, 9–13 (2015)

135. X. Zou, G. Li, Q. Wang, D. Tang, B. Wu, X. Wang, Energy storage properties of selectively functionalized Cr-group MXenes. Comput. Mater. Sci. **150**, 236–243 (2018)

136. Y. Yue, Fe2C monolayer: an intrinsic ferrimagnetic MXene. J. Magn. Magn. Mater. **434**, 164–168 (2017)

137. M. Khazaei et al., Novel electronic and magnetic properties of two-dimensional transition metal carbides and nitrides. Adv. Funct. Mater. **23**, 2185–2192 (2013)

138. H. Kumar, N.C. Frey, L. Dong, B. Anasori, Y. Gogotsi, V.B. Shenoy, Tunable magnetism and transport properties in nitride MXenes. ACS Nano **11**, 7648–7655 (2017)

139. J.-C. Lei, X. Zhang, Z. Zhou, Recent advances in MXene: preparation, properties, and applications. Front. Phys. **10**, 276–286 (2015)

140. L. Qalyoubi, A. Al-Othman, S. Al-Asheh, K. Shirvanimoghaddden, R. Mahmoodi, M. Naeble, Textile based biochar for the removal of ciprofloxacin antibiotics from water. Emergent Mater. (2023)

141. S.A.L. Bachmann, K.G.P. Nunes, T. Calvete, L.A. Feris, Low cost adsorbents prepared from brewer's spent grain for pollutants removal. Emergent Mater. **6**, 741–753 (2023)

142. D.R. Eddy, M.D. Permana, L.K. Sakti, D. Dwiyanti, T. Takei, N. Kumada, I. Rahayu, Comparative studies of synthesis of Ag/Ag2O nanoparticles by Sol-gel and sonochemical method as removal of Cr(VI). Emergent Mater. **6**, 1231–1242 (2023)

143. P. Sahay, D. Mohite, S. Arya, K. Dalmia, Z. Khan, A. Kumar, Removal of the Emergent pollutants (hormones and antibiotics) from wastewater using different kinds of biosorbent – a review. Emergent Mater. **6**, 373–401 (2023)

144. R. Kanaoujiya, S.K. Saroj, V.D. Rajput, S. Alimiddin, T. Srivastava, C.A. Minkina, M. Igwegbe, A.K. Singh, Emerging application of nanotechnology for mankind. Emergent Mater. **6**, 439–452 (2023)

145. M. El-Khomri, N. El-Messaudi, A. Dbik, S. Bentahar, Y. Fernine, A. Bouich, A. Lacherai, A. Jada, Modification of low-cost adsorbent prepared from agricultural solid waste for the adsorption and desorption of cationic dye. Emergent Mater. **5**, 1679–1688 (2022)

146. N.H. Solangi, R.R. Karri, S.A. Mazari, N.M. Mubarak, A.S. Jatoi, G. Malafaia, A.K. Azad, MXene as emerging material for photocatalytic degradation of environmental pollutants. Coord. Chem. Rev. **477**, 214965 (2023)

147. K. Li et al., Self-assembled MXene-based nanocomposites via layer-by-layer strategy for elevated adsorption capacities. Colloids Surf. A Physicochem. Eng. Asp. **553**, 105–113 (2018)

148. S. Luo et al., Preparation and dye degradation performances of self-assembled MXene-Co3O4 nanocomposites synthesized via solvothermal approach. ACS Omega **4**, 3946–3953 (2019)

149. L. Wu et al., 2D transition metal carbide MXene as a robust biosensing platform for enzyme immobilization and ultrasensitive detection of phenol. Biosens. Bioelectron. **107**, 69–75 (2018)

150. P. Zhang, M. Xiang, H. Liu, C. Yang, S. Deng, Novel two-dimensional magnetic titanium carbide for methylene blue removal over a wide pH range: insight into removal performance and mechanism. ACS Appl Mater Interfaces **11**, 24027–24036 (2019)

151. Y. Zhang, Z. Zhou, J. Lan, P. Zhang, Prediction of Ti3C2O2 MXene as an effective capturer of formaldehyde. Appl. Surf. Sci. **46**, 770–774 (2019)

152. Y. Lei et al., Facile preparation of sulfonic groups functionalized Mxenes for efficient removal of methylene blue. Ceram. Int. **45**, 17653–17661 (2019)

153. F. Meng et al., MXene sorbents for removal of urea from dialysate: a step toward the wearable artificial kidney. ACS Nano **12**, 10518–10528 (2018)

154. H. Lei et al., Insight into adsorption performance and mechanism on efficient removal of methylene blue by accordion-like V2CTx MXene. J. Phys. Chem. Lett. **11**, 4253–4260 (2020)

155. Z. Wei, Z. Peigen, T. Wubian, Q. Xia, Z. Yamei, S. ZhengMing, Alkali treated Ti3C2Tx MXenes and their dye adsorption performance. Mater. Chem. Phys. **206**, 270–276 (2018)

156. D. Vidyasagar, A. Gupta, A. Balapure, S.G. Ghugal, A.G. Shende, S.S. Umar, 2D/2D Wg-C3N4/g-C3N4 composite as "Adsorb and Shuttle" model photocatalyst for pollution mitigation. J. Photochem. Photobiol. A Chem. **370**, 117–126 (2019)

157. C. Peng et al., A hydrothermal etching route to synthesis of 2D MXene (Ti3C2, Nb2C): enhanced exfoliation and improved adsorption performance. Ceram. Int. **44**, 8886–18893 (2018)

158. M. Vakili, G. Cagnetta, J. Huang, G. Yu, J. Yuan, Synthesis and regeneration of a MXene-based pollutant adsorbent by mechanochemical methods. Molecules 24, 2478 (2019)

159. N.K. Srivastava, C.B. Majumder, Novel biofiltration methods for the treatment of heavy metals from industrial wastewater. J. Hazard. Mater. 151, 1–8 (2008)

160. A. Abbas et al., Heavy metal removal from aqueous solution by advanced carbon nanotubes: critical review of adsorption applications. Sep. Purif. Technol. 157, 141–161 (2016)

161. A.K. Fard, G. Mckay, R. Chamoun, T. Rhadfi, H. Preud'Homme, M.A. Atieh, Barium removal from synthetic natural and produced water using MXene as two dimensional (2-D) nanosheet adsorbent. Chem. Eng. J. 317, 331–342 (2017)

162. X. Feng et al., Self-assembling 2D/2D (MXene/LDH) materials achieve ultra-high adsorption of heavy metals Ni^{2+} through terminal group modification. Sep. Purif. Technol. 253, 117525 (2020)

163. B.-M. Jun, N. Her, C.M. Park, Y. Yoon, Effective removal of Pb(ii) from synthetic wastewater using Ti3C2Tx MXene. Environ. Sci. Water Res. Technol. 6, 173–180 (2020)

164. A. Shahzad et al., Mercuric ion capturing by recoverable titanium carbide magnetic nanocomposite. J. Hazard. Mater. 344, 811–818 (2018)

165. A. Shahzad et al., Two-dimensional Ti3C2Tx MXene nanosheets for efficient copper removal from water. ACS Sustain. Chem. Eng. 5, 11481–11488 (2017)

166. Y. Tang, C. Yang, W. Que, A novel two-dimensional accordion-like titanium carbide (MXene) for adsorption of Cr (VI) from aqueous solution. J. Adv. Dielectr. 8, 1850035 (2018)

167. Y. Dong, D. Sang, C. He, X. Sheng, L. Lei, Mxene/alginate composites for lead and copper ion removal from aqueous solutions. RSC Adv. 9, 29015–29022 (2019)

168. W. Mu, S. Du, Q. Yu, X. Li, H. Wei, Y. Yang, Improving barium ion adsorption on two-dimensional titanium carbide by surface modification. Dalton Trans. 47, 8375–8381 (2018)

169. Q. Peng et al., Unique lead adsorption behavior of activated hydroxyl group in two-dimensional titanium carbide. J. Am. Chem. Soc. 136, 4113–4116 (2014)

170. A. Shahzad et al., Exfoliation of titanium aluminum carbide to form nanofibers and two-dimensional nanosheets and their application in aqueous-phase cadmium sequestration. ACS Appl. Mater. Interfaces 11, 19156–19166 (2019)

171. Y. Ying et al., Two-dimensional titanium carbide for efficiently reductive removal of highly toxic chromium(VI) from water. ACS Appl. Mater. Interfaces 7, 1795–1803 (2015)

172. A. Shahzad et al., Ti3C2Tx MXene core-shell spheres for ultrahigh removal of mercuric ions. Chem. Eng. J. 368, 400–408 (2019)

173. R.P. Pandey, K. Rasool, P. Abdul Rasheed, K.A. Mahmoud, Reductive sequestration of toxic bromate from drinking water using lamellar two-dimensional Ti3C2TX (MXene). ACS Sustain. Chem. Eng. 6, 7910–7917 (2018)

174. G. Zou, J. Guo, Q. Peng, A. Zhou, Q. Zhang, B. Liu, Synthesis of urchin-like rutile titania carbon nanocomposites by iron-facilitated phase transformation of MXene for environmental remediation. J. Mater. Chem. A 4, 489–499 (2016)

175. X. Xie, C. Chen, N. Zhang, Z.-R. Tang, J. Jiang, Y.-J. Xu, Microstructure and surface control of MXene films for water purification. Nat. Sustain. 2, 856–862 (2019)

176. B.-M. Jun, M. Jang, C.M. Park, J. Han, Y. Yoon, Selective adsorption of Cs+ by MXene (Ti3C2Tx) from model low-level radioactive wastewater. Nucl. Eng. Technol. 52, 1201–1207 (2020)

177. A.R. Khan et al., Two-dimensional transition metal carbide (Ti3C2Tx) as an efficient adsorbent to remove cesium (Cs+). Dalton Trans. 48, 11803–11812 (2019)

178. L. Wang et al., Loading actinides in multilayered structures for nuclear waste treatment: the first case study of uranium capture with vanadium carbide MXene. ACS Appl. Mater. Interfaces 8, 16396–16403 (2016)

179. Y.-J. Zhang et al., Theoretical insights into the uranyl adsorption behavior on vanadium carbide MXene. Appl. Surf. Sci. 426, 572–578 (2017)

180. L. Wang et al., Rational control of the interlayer space inside two-dimensional titanium carbides for highly efficient uranium removal and imprisonment. Chem. Commun. 53, 12084–12087 (2017)

181. L. Wang et al., Efficient U(VI) Reduction and sequestration by Ti2CTx MXene. Environ. Sci. Technol. 52, 10748–10756 (2018)

182. S. Li, L. Wang, J. Peng, M. Zhai, W. Shi, Efficient thorium(IV) removal by two-dimensional Ti2CTx MXene from aqueous solution. Chem. Eng. J. 366, 192–199 (2019)

183. F. Liu et al., Preparation of Ti3C2 and Ti2C MXenes by fluoride salts etching and methane adsorptive properties. Appl. Surf. Sci. 416, 781–789 (2017)

184. W. Mu et al., Removal of radioactive palladium based on novel 2D titanium carbide. Chem. Eng. J. 358, 283–290 (2019)

185. L. Wang et al., Effective removal of anionic Re(VII) by surface-modified Ti2CTx MXene nanocomposites: implications for Tc(VII) sequestration. Environ. Sci. Technol. 53, 3739–3747 (2019)

186. H. Deng et al., Nanolayered Ti3C2 and SrTiO3 composites for photocatalytic reduction and removal of uranium(VI). ACS Appl. Nano Mater. 2, 2283–2294 (2019)

187. Z.H. Jaffari, S.-M. Lam, J.-C. Sin, H. Zeng, A.R. Mohamed, Magnetically recoverable Pd-loaded BiFeO3 microcomposite with enhanced visible light photocatalytic performance for pollutant, bacterial and fungal elimination. Sep. Purif. Technol. 236, 116195 (2020)

188. Z.H. Jaffari, S.M. Lam, J.C. Sin, A.R. Mohamed, Constructing magnetic Pt-loaded BiFeO3 nanocomposite for boosted visible light photocatalytic and antibacterial activities. Environ. Sci. Pollut. Res. 26, 10204–10218 (2019)

189. Y. Gao et al., Hydrothermal synthesis of TiO2/Ti3C2 nanocomposites with enhanced photocatalytic activity. Mater. Lett. 150, 62–64 (2015)

190. C. Peng, H. Wang, H. Yu, F. Peng, (111) TiO2-x/Ti3C2: synergy of active facets, interfacial charge transfer and Ti3+ doping for enhance photocatalytic activity. Mater. Res. Bull. 89, 16–25 (2017)

191. W. Zhou, J. Zhu, F. Wang, M. Cao, T. Zhao, One-step synthesis of Ceria/Ti3C2 nanocomposites with enhanced photocatalytic activity. Mater. Lett. 206, 237–240 (2017)

192. Q. Liu et al., MXene as a non-metal charge mediator in 2D layered CdS@Ti3C2@TiO2 composites with superior Z-scheme visible light-driven photocatalytic activity. Environ. Sci. Nano 6, 3158–3169 (2019)

193. J. Jang, A. Shahzad, S.H. Woo, D.S. Lee, Magnetic Ti3C2Tx (Mxene) for diclofenac degradation via the ultraviolet/chlorine advanced oxidation process. Environ. Res. 182, 108990 (2020)

194. S. Wu, Y. Su, Y. Zhu, Y. Zhang, M. Zhu, In-situ growing Bi/BiOCl microspheres on Ti3C2 nanosheets for upgrading visible-light-driven photocatalytic activity. Appl. Surf. Sci. 520, 146339 (2020)

195. Q. Huang, Y. Liu, T. Cai, X. Xia, Simultaneous removal of heavy metal ions and organic pollutant by BiOBr/Ti3C2 nanocomposite. J. Photochem. Photobiol. A Chem. 375, 201–208 (2019)

196. S. Vigneshwaran, C.M. Park, S. Meenakshi, Designed fabrication of sulfide-rich bi-metallic-assembled MXene layered sheets with dramatically enhanced photocatalytic performance for Rhodamine B removal. Sep. Purif. Technol. 258, 118003 (2021)

197. Y. Cui et al., Biomimetic anchoring of Fe3O4 onto Ti3C2 MXene for highly efficient removal of organic dyes by Fenton reaction. J. Environ. Chem. Eng. **8**, 104369 (2020)

198. H. Wang et al., Formation of quasi-core-shell In2S3/anatase TiO2@metallic Ti3C2Tx hybrids with favorable charge transfer channels for excellent visible-light-photocatalytic performance. Appl. Catal. Environ. **233**, 213–225 (2018)

199. C. Liu et al., Layered BiOBr/Ti3C2 MXene composite with improved visible-light photocatalytic activity. J. Mater. Sci. **54**, 2458–2471 (2019)

200. C. Cui et al., Bi2WO6/Nb2CTx MXene hybrid nanosheets with enhanced visible-light-driven photocatalytic activity for organic pollutants degradation. Appl. Surf. Sci. **505**, 144595 (2020)

201. X. Liu, C. Chen, Mxene enhanced the photocatalytic activity of ZnO nanorods under visible light. Mater. Lett. **261**, 127127 (2020)

202. Y. Diao et al., In-situ grown of g-C3N4/Ti3C2/TiO2 nanotube arrays on Ti meshes for efficient degradation of organic pollutants under visible light irradiation. Colloids Surf. A Physicochem. Eng. Asp. **594**, 124511 (2020)

203. Y. Cao et al., Fabrication of novel CuFe2O4/MXene hierarchical heterostructures for enhanced photocatalytic degradation of sulfonamides under visible light. J. Hazard. Mater. **387**, 122021 (2020)

204. S. Jiao, L. Liu, Friction-induced enhancements for photocatalytic degradation of MoS2@Ti3C2 nanohybrid. Ind. Eng. Chem. Res. **58**, 18141–18148 (2019)

205. Y. Fang, Y. Cao, Q. Chen, Synthesis of an Ag_2WO_4/Ti_3C_2 Schottky composite by electrostatic traction and its photocatalytic activity. Ceram. Int. **45**, 22298–22307 (2019)

206. H. Zhang et al., 2D a-Fe2O3 doped Ti3C2 MXene composite with enhanced visible light photocatalytic activity for degradation of Rhodamine B. Ceram. Int. **44**, 19958–19962 (2018)

207. H. Zhang, M. Li, C. Zhu, Q. Tang, P. Kang, J. Cao, Preparation of magnetic α-Fe2O3/ZnFe2O4@Ti3C2 MXene with excellent photocatalytic performance. Ceram. Int. **46**, 81–88 (2020)

208. T. Yun et al., Electromagnetic shielding of monolayer MXene assemblies. Adv. Mater. **32**, 1906769 (2020)

209. G. Redlarski et al., *The influence of electromagnetic pollution on living organisms: historical trends and forecasting changes* (Med. Res, Int, 2015)

210. B. Hocking, K.H. Mild, Guidance note: risk management of workers with medical electronic devices and metallic implants in electromagnetic fields. Int. J. Occup. Saf. Ergon. **14**, 217–222 (2008)

211. G. Nimtz, U. Panten, Broad band electromagnetic wave absorbers designed with nano-metal films. Ann. Phys. **522**, 53–59 (2010)

212. Y.-S. Choi, Y.-H. Yoo, J.-G. Kim, S.-H.J.S. Kim, A comparison of the corrosion resistance of Cu–Ni–stainless steel multilayers used for EMI shielding. Surf. Coat. Technol. **201**, 3775–3782 (2006)

213. M. Aswathi, A. Rane, A. Ajitha, Advanced materials for electromagnetic shielding: fundamentals, properties, and applications. (John Wiley & Sons, 2018)

214. P. Saini, M. Arora, Microwave absorption and EMI shielding behavior of nanocomposites based on intrinsically conducting polymers, graphene and carbon nanotubes. New polymers for special applications **3**, 73–112 (2013)

215. H.W. Ott, *Electromagnetic compatibility engineering* (John Wiley & Sons, 2011)

216. Z. Li, Z. Wang, W. Lu, B.J.M. Hou, Theoretical study of electromagnetic interference shielding of 2D MXenes films. Metals. **8**, 652 (2018)

217. P. He et al., Tailoring Ti3C2Tx nanosheets to tune local conductive network as an environmentally friendly material for highly efficient electromagnetic interference shielding. Nanoscale. **11**, 6080–6088 (2019)

218. C. Xiang et al., Lightweight and ultrathin TiO2-Ti3C2TX/graphene film with electromagnetic interference shielding. Chem. Eng. J. **360**, 1158–1166 (2019)

219. Z. Chen, X. Duan, W. Wei, S. Wang, B-J, Recent advances in transition metal-based electrocatalysts for alkaline hydrogen evolution. J. Mater. Chem. A. **7**, 14971–15005 (2019)

220. A. Parra-Puerto, K.L. Ng, K. Fahy, A.E. Goode, M.P. Ryan, A. Kucernak, Supported transition metal phosphides: activity survey for HER, ORR, OER, and corrosion resistance in acid and alkaline electrolytes. ACS Catal. **9**, 11515–11529 (2019)

221. C. Hao et al., Interface-coupling of CoFe-LDH on MXene as high-performance oxygen evolution catalyst. Mater. Today Energy. **12**, 453–462 (2019)

222. G. Fu, M. Lee, Ternary metal sulfides for electrocatalytic energy conversion. J. Mater. Chem. A. **7**, 9386–9405 (2019)

223. X. Peng et al., Recent progress of transition metal nitrides for efficient electrocatalytic water splitting. Sustain. Energy Fuels. **3**, 366–381 (2019)

224. Y. Zhu et al., Anionic defect engineering of transition metal oxides for oxygen reduction and evolution reactions. J. Mater. Chem. A. **7**, 5875–5897 (2019)

225. J.D. Benck, T.R. Hellstern, J. Kibsgaard, P. Chakthranont, T. Jaramillo, Catalyzing the hydrogen evolution reaction (HER) with molybdenum sulfide nanomaterials. ACS Catal. **4**, 3957–3971 (2014)

226. X. Zhang, X. Zhao, D. Wu, Y. Jing, Z.J.N. Zhou, High and anisotropic carrier mobility in experimentally possible Ti2 CO2 (MXene) monolayers and nanoribbons. Nanoscale. **7**, 16020–16025 (2015)

227. S. Supriya, G. Singh, R. Bahadur, A. Vinu, G. Hegde, Porous carbon derived from Arecanut seeds by direct pyrolysis for efficient CO2 capture. Emergent Mater. **5**, 1757–1765 (2022)

228. X. Wang et al., Tailoring ultrahigh energy density and stable dendrite-free flexible anode with Ti3C2Tx MXene nanosheets and hydrated ammonium vanadate nanobelts for aqueous rocking-chair zinc ion batteries. Adv. Funct. Mater. **31**, 2103210 (2021)